Reionization and cosmic microwave background distortions: A complete treatment of second-order Compton scattering

Wayne Hu, Douglas Scott, and Joseph Silk
Departments of Physics and Astronomy and Center for Particle Astrophysics, University of California, Berkeley, California 94720
(Received 7 June 1993)

The ionization history of the Universe provides a major source of ambiguity in constraining cosmological models using small angular scale microwave background anisotropies. To clarify these issues, we consider a complete treatment of Compton scattering to second order, an approach which may be applicable to other astrophysical situations. We find that only the $O(v)$ Doppler effect and the $O(v\delta)$ Vishniac effect are important for recent last scattering epochs and realistic power spectra. The $O(v^2)$ Doppler effect is not significant on any angular scale, and other higher-order effects are completely negligible. However the $O(v^2)$ effect does lead to Compton-y distortions, which, although generally below current constraints, set an unavoidable minimum level in reionization models. We consider the small-angle approximation for the Vishniac effect in detail, and show several improvements over previous treatments, particularly for low Ω_0. For standard cold dark matter models, the effect of reionization is to redistribute the anisotropies to arcminute scales; late reionization leads to partially erased primary fluctuations and a secondary contribution of comparable magnitude. Using recent anisotropy limits from the ATCA experiment, we set new constraints on baryonic dark matter models. Stronger constraints are imposed (in second order) upon models with higher Hubble constant, steeper n, and higher density. These limits depend on the specific ionization history assumed, but the factor gained by lowering the ionization fraction is generally small, and may be tested by currently planned experiments on arcminute scales.

PACS number(s): 98.70.Vc, 98.80.Es, 98.80.Hw

I. INTRODUCTION

Temperature fluctuations in the cosmic microwave background (CMB) are a direct probe of density perturbations at $z \simeq 1100$. Therefore measurements or upper limits on such fluctuations can be used to constrain cosmological models for the evolution of structure. However, there is a possible loophole at intermediate angular scales, since reionization could make the last scattering epoch more recent, and erase the small-scale fluctuations, e.g., [1]. This possibility requires significant levels of ionization back to $z \gg 10$, to reach optical depth unity at $z \ll 1100$, which is certainly feasible in some models. With the recent detection of temperature anisotropies at large angular scales by the Differential Microwave Radiometer (DMR) on the Cosmic Background Explorer (COBE) satellite [2] and stringent upper limits on intermediate angular scale fluctuations, e.g., [3], the constraining of cosmological models has entered a new phase of precision. It is becoming increasingly important to know how much leeway reionization scenarios can give for intermediate angular scale limits while not violating limits at small angular scales. In this spirit, we have attempted to systematically consider the effects of Compton scattering on CMB photons.

Primary fluctuations arising from the recombination epoch are erased on scales smaller than that subtended by the horizon at the new last scattering epoch. However, secondary fluctuations will be generated on this new surface of last scattering, mainly due to Doppler shifts among the scatterers. These secondary fluctuations are $O(v)$, except that on scales smaller than the horizon size, there is a partial cancellation of blueshifts and redshifts through a given overdense (or underdense) region. Since this new horizon scale subtends more than a degree on the sky, reionization is often invoked to save models from intermediate scale anisotropy constraints. The secondary fluctuations were therefore thought to escape any constraint until Ostriker and Vishniac [4] pointed out that a second-order contribution [of $O(v\delta)$, the so-called Vishniac term], which does not suffer from the cancellation, could be larger than the first-order term. In practice the second-order term is of the same order of magnitude as the degree-scale primary fluctuations which have erased, but occurs on arcminute scales and below.

Use of reionization to weaken anisotropy limits therefore depends on a calculation of these second-order contributions for the particular power spectrum and ionization history being considered. Detailed calculations for some models were performed by Vishniac [5] and Efstathiou [6]. However, the Vishniac term is only one of a number of possible second-order terms. Although it has been assumed that this term dominates over any others, this has not been demonstrated. Indeed, we find that the relative size of these terms depends on the matter power spectrum for the model in question. Spectra which peak above the horizon scale at last scattering produce an effect due to the scattering of anisotropic radiation which can significantly cancel the Vishniac effect. This is not the case for the cold dark matter (CDM) or isocurvature baryonic dark matter [BDM, also known as primordial isocurvature baryon (PIB)] spectra, and we

show that it is reasonable to neglect all other second-order terms, save the Vishniac term, for these models. Secondary anisotropies are therefore calculated to reasonable accuracy (in the linear regime) if the first order and Vishniac contributions to $\Delta T/T$ are evaluated. To arrive at this result, we set up in Sec. II a methodology which finds all second-order Compton scattering terms. Along the way, we uncover a number of additional physical effects which have not previously been described, e.g., minimal spectral distortions required in reionization scenarios independent of thermal history. Our general results, detailed in Appendices A and B, may also be of use for a wider range of problems. In Sec. III, we discuss the second-order contributions to anisotropy and significantly improve the approximations of Efstathiou [6]. Predictions for the CDM and BDM scenarios are computed in Sec. IV. Recent limits on arcminute scale fluctuations from the Australian Telescope Compact Array (ATCA) [7] place strong constraints on BDM models. Other studies of the effects of reionization on the microwave background [5,6] have tended to concentrate on the simplest case of a universe in which there has been no recombination. Here we have also considered the effects of more realistic ionization histories.

II. THE BOLTZMANN EQUATION FOR SECOND-ORDER COMPTON SCATTERING

A. General formalism

The Boltzmann equation in general is given by

$$\frac{\partial f}{\partial t}+\frac{\partial f}{\partial x^i}\frac{dx^i}{dt}+\frac{\partial f}{\partial \gamma_i}\frac{d\gamma_i}{dt}+\frac{\partial f}{\partial p_0}\frac{dp_0}{dt}=C(x,p)\ , \qquad (1)$$

where f is the photon occupation number, γ_i are the direction cosines for a photon of four-momentum p, and the expression $C(x,p)$ is the collision term. Latin indices range from 1 to 3, and we have employed the implicit summation convention. There are two distinct classes of second-order Boltzmann equations that we might consider. The left-hand side of Eq. (1) may be expanded to second order in metric perturbations, whereas the right-hand side, in the case of Compton scattering, may be expanded to second order in the energy transfer from collisions. In Appendix A, we carry through a full derivation of all second-order gravitational terms due to metric perturbations in the synchronous gauge. However, in this paper we are primarily interested in the effects of Compton scattering, which are constrained by causality to manifest themselves on small scales where gravitational effects are unimportant. Thus we take the zeroth-order approximation of Eq. (1) with respect to the metric fluctuations and find

$$\frac{\partial f}{\partial t}+\frac{\partial f}{\partial x^i}\frac{dx^i}{dt}-\frac{1}{a}\frac{da}{dt}p_0\frac{\partial f}{\partial p_0}=C(x,p)\ . \qquad (2)$$

The third term on the left merely expresses the cosmological redshift of the photon energy, $p_0 \propto a^{-1}$, where $a(t)$ is the usual scale factor. In the homogeneous and isotropic limit, the second term in Eq. (2) vanishes. Spectral distortions in the early Universe are often computed in this approximation (see Sec. II B). In Sec. III, we calculate the effects of dropping the assumption of homogeneity. If, on the other hand, we are only concerned with temperature and not spectral distortions, we may integrate over momentum p. The third term may thus be eliminated since temperature and energy redshift in the same manner.

The goal is to derive the collision term for Compton scattering, $\gamma(p)+e(q)\leftrightarrow\gamma(p')+e(q')$, to second order in the small energy transfer due to scattering. Note that we are performing calculations in the *linear* regime. Thus, the results are of interest only when the effects of the first-order terms suffer cancellation, as in the case of a thick last scattering surface. The lowest-order term is then of second order. Third- and higher-order effects are therefore negligible as long as the second-order term is not canceled. Mixed-order coupling (i.e., first to third) is also insignificant. We discuss these effects in detail in Sec. III.

Our approach may be of more general interest since it provides a coherent framework for all Compton scattering effects, be they spectral distortions or anisotropies. In the proper limits, the equation derived below reduces to familiar equations and effects, e.g., the Kompaneets equation (Sunyaev-Zel'dovich effect), linear Doppler equation (Vishniac effect). Furthermore, new truly second-order effects such as the $O(v^2)$ quadratic Doppler effect are obtained. These effects predict distortions well below the observational limits obtainable today. In principle, however, the fact that they may mix both anisotropies and spectral distortions makes them distinguishable.

We make the following assumptions in deriving the equations: (1) the Thomson limit applies, i.e., the fractional energy transfer $\delta p/p \ll 1$ in the rest frame of the background radiation; (2) the radiation is unpolarized and remains so; (3) the density of electrons is low so that Pauli suppression terms may be ignored; and (4) the electron distribution is thermal about some bulk flow velocity $\mathbf{v}$. Approximations (1), (3), and (4) are valid for most situations of cosmological interest. The approximation regarding polarization could be dropped to give coupled equations for perturbations in the total and polarized components [8]. Polarization perturbations are typically an order of magnitude smaller than temperature distortions [9]. Thus the contribution from polarization to the evolution of *temperature* distortions is a small effect, as the microwave background never generates a significant polarization. For calculations on the generation of polarization in second-order theory, see [6].

The collision term may in general be expressed as [10]

$$C(\mathbf{x},\mathbf{p})=\frac{1}{2E(p)}\int DqDq'Dp'(2\pi)^4\delta^{(4)}(p+q-p'-q')|M|^2$$
$$\times\{g(\mathbf{x},\mathbf{q}')f(\mathbf{x},\mathbf{p}')[1+f(\mathbf{x},\mathbf{p})]-g(\mathbf{x},\mathbf{q})f(\mathbf{x},\mathbf{p})[1+f(\mathbf{x},\mathbf{p}')]\}\ , \qquad (3)$$

where $|M|^2$ is the Lorentz-invariant matrix element, $f(\mathbf{x},\mathbf{p})$ is the photon distribution function, $g(\mathbf{x},\mathbf{q})$ is the electron distribution function, and

$$Dq=\frac{d^3q}{(2\pi)^3 2E(q)}$$

is the Lorentz-invariant phase space element. The terms in (3) which contain the distribution functions are just the contributions from scattering into and out of the momentum state $\mathbf{p}$ including stimulated emission effects.

We will assume that the electrons are thermally distributed about some bulk flow velocity $\mathbf{v}$:

$$g(\mathbf{x},\mathbf{q})=(2\pi)^3 n_e(\mathbf{x})[2\pi m T_e]^{-3/2}\exp\left\{\frac{-[\mathbf{q}-m\mathbf{v}(\mathbf{x})]^2}{2mT_e}\right\}, \tag{4}$$

where m is the electron mass, and we employ units with $c=\hbar=k=1$. Expressed in the rest frame of the electron, the matrix element for Compton scattering summed over polarization is given by [11]

$$|M|^2=2(4\pi)^2\alpha^2\left[\frac{\tilde{p}'}{\tilde{p}}+\frac{\tilde{p}}{\tilde{p}'}-\sin^2\tilde{\beta}\right], \tag{5}$$

where the tilde denotes quantities in the rest frame of the electron, α is the fine structure constant, and $\cos\tilde{\beta}=\tilde{\gamma}\cdot\tilde{\gamma}'$ is the scattering angle. Note that here and below we define $p\equiv p_0=|\mathbf{p}|$. Of course, the matrix element must be expressed in terms of the corresponding quantities in the frame of the radiation for calculational purposes [see Eq. (B1)].

The result of integrating over the electron momenta can be written

$$C(\mathbf{x},\mathbf{p})=n_e\sigma_T\int dp'\frac{p'}{p}\int\frac{d\Omega'}{4\pi}\frac{3}{4}[C_0+C_{p/m}+C_v+C_{vv}+C_{T_e/m}+C_{vp/m}+C_{(p/m)^2}], \tag{6}$$

where we have kept terms to second order in $\delta p/p$. The explicit expressions for the quantities in Eq. (6) are given in Eqs. (B4) and (B5) of Appendix B and are discussed in turn below. This equation may be considered as the source equation for all first- and second-order Compton scattering effects. However, in most cases of interest only a few of these terms will ever contribute. We have therefore written the collision equation implicitly and expressed it in terms of the scaling behavior of the contributing elements.

The expansion of the Compton collision term to second order in $\delta p/p$ has actually involved *several* small quantities. It is worthwhile to compare these terms. The quantity T_e/m characterizes the kinetic energy of the electrons and is to be compared with p/m or essentially T/m where T is the temperature of the photons. Before a redshift $8.0(\Omega_0 h^2)^{1/5}x_e^{-2/5}$, where x_e is the ionization fraction [this corresponds to $z\gtrsim 500(\Omega_B h^2)^{2/5}$ for standard recombination], the tight coupling between photons and electrons via Compton scattering requires these two temperatures to be comparable. At lower redshifts, it is possible that $T_B \gg T$, which produces distortions in the radiation via the Sunyaev-Zel'dovich (SZ) effect as discussed further below. For the reionization scenarios which we consider, these two temperatures will typically still be comparable at last scattering, $z_*\simeq 50$ with $T/m \simeq 5\times 10^{-10}(1+z_*)$. The SZ effect, however, will play a role at lower redshifts even in these scenarios. Note that the term T_e/m may also be thought of as the average thermal velocity squared $\langle v_{\rm th}^2\rangle = 3T_e/m$. This is to be compared with the bulk velocity squared v^2 and will depend on the specific means of ionization. The bulk velocity is related to the fractional overdensity $\delta\equiv\delta\rho/\rho$ by the continuity equation. On scales much smaller than the horizon, $v\ll\delta$ in linear theory.

It is appropriate at this point to examine the physical significance and qualitative features of each of the sources in the collision term of Eq. (6).

1. C_0: *Anisotropy suppression*

In the absence of electron motion, there is no preferred direction. Thus to zeroth order, scattering makes the radiation distribution more isotropic. The C_0 term given by Eq. (B4) of Appendix B indeed equalizes the distribution function over all directions via scattering into and out of a given mode. It is therefore responsible for the suppression of primordial anisotropies as seen by the scatterers. It can also significantly affect the regeneration of *inhomogeneities* when ordinary contributions are suppressed, as in the case of thick last scattering surfaces (Sec. III D). Recall that an inhomogeneity on the last scattering surface becomes an anisotropy in the CMB today.

2. C_v *and* C_{vv}: *Linear and quadratic Doppler effect*

Aside from the small electron recoil (see Sec. II A 3), the kinematics of Thomson scattering require that no energy be transferred in the rest frame of the electron, i.e., $\tilde{p}'=\tilde{p}$. Nevertheless, the transformation into the background frame induces a Doppler shift, so that

$$\frac{\delta p}{p}=\frac{1-\mathbf{v}\cdot\boldsymbol{\gamma}}{1-\mathbf{v}\cdot\boldsymbol{\gamma}'}-1$$
$$=\mathbf{v}\cdot(\boldsymbol{\gamma}'-\boldsymbol{\gamma})+(\mathbf{v}\cdot\boldsymbol{\gamma}')\mathbf{v}\cdot(\boldsymbol{\gamma}'-\boldsymbol{\gamma})+O(v^3). \tag{7}$$

Notice that in addition to the usual linear term in v, there is also a term quadratic in v.

To gain physical insight into these Doppler effects, we can approximate the photons as isotropic and neglect the

angular dependence of Thomson scattering (we will postpone discussion of the precise effects until Sec. III). Averaging over the incoming direction γ, we obtain

$$\left\langle \frac{\delta p}{p} \right\rangle \simeq \mathbf{v}\cdot\boldsymbol{\gamma}' + (\mathbf{v}\cdot\boldsymbol{\gamma}')^2 . \tag{8}$$

Thus the linear Doppler effect introduces an energy shift whose sign depends on direction, whereas the quadratic Doppler effect, which is positive definite, always gives rise to a blueshift of the photons.

Now let us consider the case where there are many scattering blobs, so that the directions of the electron velocities are in effect randomized. In this case, the net linear effect vanishes and

$$\left\langle \frac{\delta p}{p} \right\rangle \simeq \frac{1}{3}\langle v^2 \rangle ; \tag{9}$$

i.e., since redshifts and blueshifts cancel, there is no net transfer of energy to the photons to first order in v. The quadratic Doppler term, however, represents a net energy gain of

$$\Delta \equiv \frac{\delta \mathcal{E}}{\mathcal{E}} = \frac{4}{3}\langle v^2 \rangle , \tag{10}$$

since the energy density $\mathcal{E} \propto T^4$, and the Doppler shift of a blackbody is a blackbody with $T = T_0(1+\delta p/p)$. Here, we assume for simplicity that all the photons in the spectrum scattered once.

These effects are not wholly equivalent to a uniform Doppler shift. In averaging over angles above, we have really superimposed many Doppler shifts for individual scattering events. Therefore the resulting spectrum is a superposition of blackbodies with a range of temperatures $\Delta T/T = O(v)$. Zel'dovich, Illarionov, and Sunyaev [12] have shown that this sort of superposition leads to spectral distortions of the Compton-y type with $y = O(v^2)$. Thus, spectral distortions have a quadratic dependence on v and may be considered as part of the quadratic Doppler effect.

In summary, the linear Doppler effect is primarily canceled after many scatterings. Nevertheless, some residual effects remain due to the evolution of the electron velocities and densities during the last scattering epoch [13] and the increased probability of scattering in an overdense region [4]. The quadratic Doppler effect leads to an average net energy increase of $\Delta \simeq \frac{4}{3}\tau\langle v^2 \rangle$, and a spectral distortion of the Compton-y type. Here $\tau = \int n_e \sigma_T dt$ is the optical depth, which gives the fraction of photons scattered if $\tau \ll 1$. We will now see that the quadratic Doppler effect for bulk flows is in fact entirely equivalent to the Sunyaev-Zel'dovich effect for thermal motions.

3. $C_{T_e/m}$ and $C_{p/m}$: Thermal Doppler effect and recoil

Of course, we have artificially separated out the bulk and thermal components of the electron velocity. The thermal velocity leads to a quadratic Doppler effect exactly as described above if we make the replacement $\langle v^2 \rangle \to \langle v_{\rm th}^2 \rangle = 3T_e/m$ [e.g., in Eq. (10)]. For an isotropic distribution of photons, this leads to the familiar Sunyaev-Zel'dovich (SZ) effect [14]. The SZ effect can therefore be understood as the second-order spectral distortion and energy transfer due to the superposition of Doppler shifts for individual scattering events off electrons in thermal motion. This can also be naturally interpreted macrophysically: hot electrons transfer energy to the photons via Compton scattering. Spectral distortions result since low energy photons are shifted upward in frequency, leading to the Rayleigh-Jeans depletion and the Wien tail enhancement characteristic of Compton-y distortions. The fractional energy change due to scattering is

$$\Delta \simeq 4y \simeq \tfrac{4}{3}\tau\langle v_{\rm th}^2 \rangle . \tag{11}$$

Note that the thermal and quadratic Doppler effects are wholly equivalent in this sense.

Even though this is a net energy gain, the effective temperature in the Rayleigh-Jeans region is suppressed due to photon depletion (up scattering):

$$\left[\frac{\Delta T}{T}\right]_{{\rm RJ},y} = -2y \simeq -\frac{\Delta}{2} . \tag{12}$$

This is to be distinguished from the linear Doppler effect, which provides a frequency-independent shift in temperature given by $\Delta T/T \simeq \Delta/4$ (cf. Sec. II A 2).

If the photons have energies comparable to the electrons (i.e., the electron and photon temperatures are nearly equal), there is also a significant correction due to the recoil of the electron. The scattering kinematics tell us that

$$\frac{\tilde{p}'}{\tilde{p}} = \left[1 + \frac{\tilde{p}}{m}(1-\cos\tilde{\beta})\right]^{-1} . \tag{13}$$

Thus to lowest order, the recoil effects are $O(p/m)$. Together with the thermal Doppler effect, these terms form the familiar Kompaneets equation [15] in the limit where the radiation is isotropic (as described in Sec. II B). The combination of thermal Doppler shift and recoil drive the photons to a Bose-Einstein distribution of temperature T_e. A blackbody distribution cannot generally be established since Compton scattering requires conservation of photon number.

4. $C_{vp/m}$ and $C_{(p/m)^2}$: Higher-order recoil effects

These terms represent the next order in corrections due to the recoil effect. In almost all cases, they are entirely negligible. Specifically, for the CMB, when electron bulk flow effects become significant $(p/m) \leq O(v^2)$. Furthermore, since there is no cancellation in the $C_{p/m}$ term, $C_{(p/m)^2}$ will never produce the dominant effect. We will hereafter drop these terms in our consideration.

B. The isotropic limit and spectral distortions

Even for an initially anisotropic radiation field, multiple scattering off electrons will have the zeroth-order effect of erasing the anisotropy (see Sec. II A 1). New anisotropies will be generated primarily at the last scatter-

ing event. Therefore at epochs in which the optical depth is high, we can approximate the radiation field as nearly isotropic. We will treat the case of the anisotropy developed during the last scattering epoch in Sec. III. Note that the general results of Appendix B can be employed to study the effects of Compton scattering on highly anisotropic radiation. For example, Eq. (B4) contains the anisotropic generalization of the Kompaneets equation which may be useful in other astrophysical settings.

Under the additional assumption of isotropy, the collision term becomes more tractable and transparent:

$$C(\mathbf{x},\mathbf{p})=n_e\sigma_T\left\{-\boldsymbol{\gamma}\cdot\mathbf{v}p\frac{\partial f}{\partial p}+\left[[(\boldsymbol{\gamma}\cdot\mathbf{v})^2+v^2]p\frac{\partial f}{\partial p}+\left[\frac{3}{20}v^2+\frac{11}{20}(\boldsymbol{\gamma}\cdot\mathbf{v})^2\right]p^2\frac{\partial^2 f}{\partial p^2}\right]\right.$$
$$\left.+\frac{1}{mp^2}\frac{\partial}{\partial p}\left[p^4\left[T_e\frac{\partial f}{\partial p}+f(1+f)\right]\right]\right\}. \tag{14}$$

The first and second terms represent the linear and quadratic Doppler effects, respectively. The final term is the usual Kompaneets equation.

Notice that in the limit of many scattering blobs (or equivalently the multiple scattering limit), we can average over the direction of the electron velocity. The first-order linear Doppler effect primarily cancels in this case and we can reduce Eq. (14) to

$$C(\mathbf{x},p)=n_e\sigma_T\left\{\frac{\langle v^2\rangle}{3}\frac{1}{p^2}\frac{\partial}{\partial p}\left[p^4\frac{\partial f}{\partial p}\right]+\frac{1}{mp^2}\frac{\partial}{\partial p}\left[p^4\left[T_e\frac{\partial f}{\partial p}+f(1+f)\right]\right]\right\}. \tag{15}$$

Under the replacement $\langle v_{\rm th}^2\rangle=3T_e/m\rightarrow v^2$, the SZ (thermal Doppler) portion of the Kompaneets equation and quadratic Doppler equation have the same form. We also regain the factor of $\frac{1}{3}$ described in (9). Thus, spectral distortions due to bulk flow have exactly the same form as SZ distortions and can be characterized by the Compton-y parameter given in its full form by

$$y=\int n_e\sigma_T\left[\frac{1}{3}\langle v^2(t)\rangle+\frac{T_e-T}{m}\right]dt\ . \tag{16}$$

A full analysis of the Boltzmann equation analogous to that performed in Sec. III yields this result as well. The appearance of the photon temperature T in Eq. (16) is due to the recoil terms in the Kompaneets equation [cf. Eq. (11)].

As was noted by Zel'dovich and Sunyaev [16] the observational constraints on the Compton-y parameter, in conjunction with other spectral limits, can rule out some reionization histories independently of the detailed thermal history of the models. However, Bartlett and Stebbins [17] show that for a low Ω_B universe as implied by nucleosynthesis, no such model-independent constraints exist. Furthermore, for the case where the electron and photon temperatures are equal, there is no SZ effect as one can clearly see from Eq. (16). Therefore, the bulk flow effect places a lower limit on spectral distortions due to any given reionization history (although we expect the SZ effect to dominate for most realistic schemes).

For example in an $\Omega_0=1$ universe with full ionization up to a redshift z_i and $T_e=T$,

$$y\simeq 4.1\times10^{-2}(\Omega_B h)[(1+z_i)^{1/2}-1]\langle v_0^2\rangle\ , \tag{17}$$

where $\langle v_0^2\rangle$ is the (spatially) averaged square of the velocity today. Here and throughout the paper Ω_B refers to the fraction of the critical density *of the intergalactic medium* in baryons; it does not include baryonic matter in compact objects. We have assumed linear growth of velocities in an $\Omega_0=1$ universe:

$$v(k,\eta)=i\frac{\dot\delta}{k}=\frac{2i\delta}{k\eta}\propto\eta\quad[\Omega_0=1]\ , \tag{18}$$

where the overdot denotes a derivative with respect to conformal time $\eta=\int dt/a$. Given a power spectrum $P(k)$ for the baryon density fluctuations, we can compute the average velocity as

$$\langle v_0^2\rangle=\frac{2V_x}{(\pi\eta_0)^2}\int dk\,P(k,\eta_0)\ , \tag{19}$$

assuming ergodicity. Here V_x is the volume in which the universe is assumed to be periodic. The result for the standard cold dark matter (CDM) scenario, normalized to the COBE measurement [2], is therefore $v_{0,\rm rms}=1100$ km/s assuming that the baryons follow the dark matter distribution (see Sec. V for details). Note that this value is rather large, since COBE requires a bias factor $b\simeq1$ which produces excessive small-scale velocities. For comparison purposes, the sun's velocity with respect to the CMB is 365 ± 18 km/s whereas the velocity of the Local Group is 622 ± 20 km/s [18]. The upper limit on the Compton-y distortion from the Far Infrared Absolute Spectrophotometer (FIRAS) [19] is $y<2.5\times10^{-5}$. Therefore it is appropriate to reexpress Eq. (17) as

$$z_{\rm max}\simeq3.0\times10^3\left[\frac{y}{2.5\times10^{-5}}\right]^2\left[\frac{1000\ {\rm km/s}}{v_{0,\rm rms}}\right]^4\frac{1}{(\Omega_B h)^2}\ , \tag{20}$$

where $z_{\max}$ is the maximum redshift at which the electrons can be fully ionized.

However, our assumption that the electron density follows the dark matter is invalid at high redshifts. At redshifts $z > z_{\rm drag} \simeq 160(\Omega_0 h^2)^{1/5} x_e^{-2/5}$, Compton drag on the electrons and protons prevents matter from falling into the dark matter wells. Thus, (20) will not give a constraint if $z_{\max} > z_{\rm drag}$. Correspondingly, the prediction for CDM is $y(z_{\rm drag}) \simeq 3 \times 10^{-7}$, almost two orders of magnitude below the current limits. Almost certainly, foreground contamination from hot clusters will make this effect unobservable. Estimates employing cluster modeling yield $y \simeq 2\text{–}6 \times 10^{-6}$, but are extremely sensitive to the normalization of the power spectrum and cluster dynamics [20]. Therefore in flat $\Omega_0 = 1$ models, the quadratic Doppler effect does not yield a measurable average (isotropic) Compton-y parameter. In Sec. III F, we calculate the fluctuations in the Compton-y parameter at arcminute scales and show that it too is negligible. Note that the isotropic Compton-y distortion is an integral over optical depth $d\tau$; i.e., it has a contribution from all scatterings. On the other hand, correlations (i.e., temperature fluctuations) come from an integral over the visibility function $\exp(-\tau) d\tau$, i.e., they are dominated by the last scattering event.

The $O(v^2)$ Compton-y distortion is non-negligible in the case of open universes. In an open universe, velocities grow more slowly so that they are still reasonably large at the scattering epoch. Furthermore, last scattering happens at lower redshifts for baryon-dominated open models. In models with relatively low Ω_B, predictions for the quadratic Doppler effect are comparable to estimates of the cluster SZ effect, although still below the present constraints. If the intergalactic medium has been collisionally or photoionized, the average thermal SZ effect will generally be larger than the quadratic Doppler effect; higher Ω_B models with early ionization of this type can already be ruled out from their larger thermal y distortion (see, e.g., [21]). However, it is worthwhile to note that quadratic Doppler distortions are the minimum required in the case of reionization and unlike the SZ effect do not suffer from uncertainties in ionization mechanisms or cluster dynamics.

III. SMALL-SCALE BRIGHTNESS FLUCTUATIONS

A. The sources of brightness fluctuations

Having shown that spectral distortions are minimal and simply described by the Compton-y parameter, we will concentrate on temperature anisotropies; i.e., we shall no longer be concerned with frequency dependence. Therefore let us integrate the distribution over frequencies to obtain the fractional energy, or *brightness,* perturbation to the spectrum $\Delta \equiv \delta\mathcal{E}/\mathcal{E}$ [22]. It is appropriate at this point to specialize our discussion of the sources for the case of weakly anisotropic brightness fluctuations in an inhomogeneous universe.

1. $O(\Delta - \Delta_0)$: *Anisotropy suppression in the presence of sources*

The C_0 term in Eq. (6) reduces anisotropies. The anisotropy can be expressed as $\Delta - \Delta_0$ where

$$\Delta_l = \int \frac{d\Omega'}{4\pi} P_l(\mu') \Delta \tag{21}$$

are the Legendre moments of the brightness fluctuation. For future reference, note that we take μ to be defined with respect to the symmetry axis x_3, $\mu = \boldsymbol{\gamma} \cdot \hat{\mathbf{x}}_3$. We assume that for plane wave situations there is an azimuthal symmetry about the direction of the wave vector $\hat{\mathbf{x}}_3$, since to lowest order the source term possesses this symmetry (see [23] and Sec. III D).

The anisotropy suppression term plays an interesting role when in the presence of another source that generates an anisotropy. For example, the first-order Doppler term generates a local dipole anisotropy of order

$$\Delta - \Delta_0 \simeq \int (4\mathbf{v} \cdot \boldsymbol{\gamma}) d\tau \ ,$$

since photons are blueshifted in the direction of the electron velocity and redshifted in the opposite direction. However, we know that this cannot continue to be true for arbitrarily high optical depth. The Doppler anisotropy saturates precisely at $\Delta - \Delta_0 = 4\mathbf{v} \cdot \boldsymbol{\gamma}$ since once all the photons have been scattered, further scattering has no effect. This is easy to see in the electron rest frame. Here the photons are now isotropic and scattering changes only the direction, not the magnitude of their momentum. This constraint on the anisotropy is imposed by the anisotropy suppression term. When the anisotropy reaches its maximum allowable magnitude, this term exactly cancels the source of the anisotropy. We shall now see that it can also play a significant role in second-order theory.

2. $O(v\delta)$ *and* $O([\Delta - \Delta_0]\delta)$: *Scattering in overdense regions*

In a universe growing ever more inhomogeneous via gravitational instability, there are additional effects due to the enhanced probability of Compton scattering off overdense regions caused by the increase in the electron number density:

$$n_e = x_e(\eta)(1 - Y_p/2) n_B(\mathbf{x}, \eta) = \bar{n}_e(\eta)[1 + \delta(\mathbf{x}, \eta)] \ , \tag{22}$$

where Y_p is the primordial mass fraction in helium, x_e is the ionization fraction (assumed to be independent of position), n_B is the baryon number density, and δ is the fractional overdensity in baryons [24].

The overdensity δ, which is of first order in perturbation theory, couples with ordinary first-order terms to produce effectively second-order terms. Therefore, there are two possible additional terms of $O(v\delta)$ and $O([\Delta - \Delta_0]\delta)$. The former is the Vishniac term.

The Vishniac effect operates since in an overdense region there is an increased probability of scattering and inducing a Doppler shift. This leads to a brightness fluctuation on the scale of the overdense region δ. Of course, just as in the first-order effect, this mechanism cannot operate once all the photons have already scattered. If

scattering has already taken place in the underdense regions, the increase in probability of scattering off overdense regions can have no effect. Again the end result is an anisotropy of order $\Delta-\Delta_0=4\mathbf{v}\cdot\boldsymbol{\gamma}$ with no small-scale fluctuations in the brightness. This limitation is of course handled by the $O([\Delta-\Delta_0]\delta)$ term. If $\Delta-\Delta_0$ reaches the maximum allowable magnitude of $4\mathbf{v}\cdot\boldsymbol{\gamma}$, it will erase the Vishniac effect. In the presence of an anisotropy, the increase in probability of scattering off overdense regions causes an enhanced *reduction* of the anisotropy in those regions via the anisotropy suppression term. Of course, this term is also present even in the absence of sources such as the Vishniac effect. In the case where the incident radiation is anisotropic and the electrons stationary, this effect describes the preferential erasure of the anisotropy in overdense regions. It would then actually *generate* small-scale brightness fluctuations while simultaneously *reducing* the anisotropy. However, in the present case of interest, this term operates by placing a physically necessary constraint on the Vishniac effect.

When is this constraint important? Notice that the anisotropy suppression term is only effective in the presence of a significant anisotropy $\Delta-\Delta_0$. However, for velocities on a scale much smaller than the thickness of the last scattering surface, the cancellation of redshifts and blueshifts guarantees that no such anisotropy can be established. Thus it is only if the velocities which generate the Vishniac effect are on the scale of (or larger than) the thickness of the last scattering surface that it can be canceled by the $O([\Delta-\Delta_0]\delta)$ anisotropy suppression term. We find that for the CDM and BDM models discussed later, this is not the case, and the $O([\Delta-\Delta_0]\delta)$ term may be dropped. However, it would be possible *in principle* to have a power spectrum which peaks on horizon size scales, and then the anisotropic effect would be important for eliminating the Vishniac effect arising from velocities on these scales, as physically required.

3. *The second-order brightness equation*

Now let us write down the equation expressing the evolution of the brightness under the above-mentioned sources. Integrating both sides of the Boltzmann equation [Eqs. (2) and (6)] over the spectrum, we obtain the brightness equation to second order:

$$\dot{\Delta}+\gamma_i\partial_i\Delta=\bar{n}_e\sigma_T a[1+\delta(\mathbf{x})]\times\{\Delta_0-\Delta+\tfrac{1}{2}P_2(\mu)\Delta_2+4\boldsymbol{\gamma}\cdot\mathbf{v}-v^2+7(\boldsymbol{\gamma}\cdot\mathbf{v})^2+O([\Delta_0-\Delta]v)\}\ , \tag{23}$$

where the overdot represents a conformal time derivative. Notice the presence of the effects described in Secs. III A 1 and III A 2. The $O(\Delta-\Delta_0)$ term represents the anisotropy suppression. In the case when $\Delta-\Delta_0$ has reached its maximum of $\Delta-\Delta_0=4\mathbf{v}\cdot\boldsymbol{\gamma}$, it cancels both the first-order Doppler and the Vishniac terms. The Δ_2 term arises since we employ the true angular dependence of Compton scattering. This does not affect the qualitative picture, however.

The $O([\Delta-\Delta_0]v)$ term has been left implicit. We will show that the $O(v^2)$ term itself is negligible. Therefore, since on all scales of interest $\Delta-\Delta_0\lesssim v$ and the equations governing the two are similar, these terms are negligible as well. We have also assumed that the cluster SZ effect is unimportant at the last scattering epoch. The average SZ effect will produce an isotropic Compton-y distortion and have no effect on small scale anisotropies.

We can rewrite Eq. (23) implicitly as

$$\dot{\Delta}+\gamma_i\partial_i\Delta+\dot{\tau}(\eta)\Delta=\dot{\tau}(\eta)S(\mathbf{x},\boldsymbol{\gamma},\eta)\ , \tag{24}$$

where the conformal time derivative of the optical depth, $\dot{\tau}(\eta)=\bar{n}_e\sigma_T a$, can be interpreted as the probability of scattering in the interval $d\eta$. Note that the source term $S(\mathbf{x},\boldsymbol{\gamma},\eta)$ includes the anisotropy suppression (Δ_0) part. The first-order term generates fluctuations which are canceled by opposing fluctuations as the photons travel the full length of the perturbation. However, the anisotropy suppression term acts to rescatter the photons into the direction that avoids such cancellation. This of course reduces the local anisotropy of the brightness at the expense of its small-scale inhomogeneity. We will make this argument more concrete in Sec. III D.

B. General formalism and definitions

To solve the brightness equation (24), we transform to its Fourier space analogue,

$$\Delta(\mathbf{k},\boldsymbol{\gamma},\eta)=\frac{1}{V_x}\int d^3x\ \Delta(\mathbf{x},\boldsymbol{\gamma},\eta)\exp(-i\mathbf{k}\cdot\mathbf{x})\ , \tag{25}$$

which has the well known solution [6]

$$\Delta(\mathbf{k},\boldsymbol{\gamma},\eta)=\int_0^\eta S(\mathbf{k},\boldsymbol{\gamma},\eta')g(\eta,\eta')\exp[ik\mu(\eta'-\eta)]d\eta'\ , \tag{26}$$

where $\mu=\boldsymbol{\gamma}\cdot\mathbf{k}/k$ and

$$g(\eta,\eta')=\dot{\tau}(\eta)\exp\left[-\int_{\eta'}^{\eta}d\eta''\dot{\tau}(\eta'')\right]\equiv\frac{d}{d\eta'}\exp[-\tau(\eta,\eta')] \tag{27}$$

is the so-called visibility function [note that $g(\eta,\eta)=\dot{\tau}(\eta)$]. For the case of full ionization where $x_e=1$,

$$\tau(z=0,z)=\frac{\sigma_T H_0}{4\pi G m_p}(1-Y_p/2)\frac{\Omega_B}{\Omega_0^2}[2-3\Omega_0+(1+\Omega_0 z)^{1/2}(\Omega_0 z+3\Omega_0-2)]\ , \tag{28}$$

(where m_p is the mass of the proton) or, alternatively,

$$\tau(\eta_0,\eta)=\frac{\sigma_T H_0}{4\pi G m_p}(1-Y_p/2)\frac{\Omega_B}{\Omega_0^2}\left\{2-3\Omega_0-(1-\Omega_0)^{3/2}\coth\left[\frac{\eta}{2\mathcal{R}}\right]\left[3-\coth^2\left[\frac{\eta}{2\mathcal{R}}\right]\right]\right\}\ , \tag{29}$$

for $\Omega_0<1$, where $\mathcal{R}=H_0^{-1}(1-\Omega_0)^{-1/2}$ is the curvature scale today, which merely translates our convention for conformal time to the usual development angle $\Psi=\eta/\mathcal{R}$. For $\Omega_0=1$, the expression in braces should be replaced by $\{(\eta_0/\eta)^3-1\}$.

We are primarily interested in the solution at small wavelengths, i.e., $k\,\delta\eta\gg1$ where $\delta\eta$ is the conformal time "thickness" of the last scattering surface, located at η_*. The precise definition of η_* is somewhat arbitrary, e.g., η_* could be defined as the epoch at which optical depth becomes unity (we will employ this definition unless otherwise stated). For late last scattering $\delta\eta\simeq\eta_*$; it is in this sense that we mean the last scattering surface for reionization scenarios is "thick."

Neglecting the evolution of the source term and the optical depth, the integral over the plane wave for $\mu\neq0$ in Eq. (26) will in general cancel except for a small portion of the order of a wavelength. Therefore the resulting brightness fluctuations will be of order

$$\Delta(\mathbf{k},\gamma,\eta)\simeq S(\mathbf{k},\gamma,\eta)\tau_\lambda(\eta),\quad \mu\neq0\ , \tag{30}$$

where $\tau_\lambda=(2\pi/k)\dot\tau(\eta)$ is the optical depth across one wavelength. If the perturbation has many wavelengths over the last scattering surface, $\tau_\lambda\ll1$ since the optical depth across the whole surface is of order unity. Therefore, the brightness fluctuations are suppressed as compared with the source terms, i.e., $\Delta(k)\ll v(k)$ for $k\eta_*\gg1$.

The $\mu=0$ mode escapes this cancellation. Thus the brightness fluctuation has a significant value only if the wave vector $\mathbf{k}$ is perpendicular to the direction of the photon momentum, γ. The interpretation of this statement is simply that if the wave vector were not strictly perpendicular to the photon momentum vector, photons in a given direction would have scattered off both crests and troughs of the perturbation, yielding net cancellation.

In the case of the first-order (linear Doppler) term, $S(\mathbf{k},\gamma,\eta)=4\gamma\cdot\mathbf{v}=4\mu v$, which vanishes for the $\mu=0$ mode. Therefore, as pointed out by Kaiser [13], the first-order term is primarily canceled up to a factor which involves the time evolution of the perturbation. It is important, however, to note that the general cancellation argument holds for *any* source term, while near perfect cancellation will occur for $S(\mathbf{k},\mu=0,\eta)=0$.

Having determined which perturbation modes give large contributions to brightness fluctuations, we need to translate this information into the temperature fluctuations on the sky today. First we must relate the brightness distortion Δ to a fractional temperature perturbation. For linear Doppler effects which change the temperature uniformly across the spectrum and leave it as a blackbody, $\Delta\simeq4\Delta T/T$. Quadratic and thermal Doppler effects create Compton-y distortions such that $\Delta\simeq-2(\Delta T/T)_{\rm RJ}$ [see Eq. (12)]. To keep the expression applicable to both sorts of distortions, we will write

$$\frac{\Delta T}{T}=\frac{K}{4}\Delta\ , \tag{31}$$

where $K=1$ for the linear Doppler effect and $K=-2$ for quadratic and thermal Doppler terms (Compton-y distortions).

We will use the small-angle approximation given by Doroshkevich, Zel'dovich, and Sunyaev [25] for the *observed* mean squared temperature fluctuation:

$$\left[\frac{\Delta T}{T}\right]^2=\frac{V_x}{32\pi^2}\int_0^\infty k^2dk\frac{K^2}{2}\int_{-1}^{1}d\mu|\Delta(k,\mu,\eta)|^2\times W(kR_\eta(1-\mu^2)^{1/2})\ , \tag{32}$$

where $W(q)$ is the experimental window function, $q=kR_\eta(1-\mu^2)^{1/2}\simeq l$ (i.e. the multipole number) at small scales, and R_η translates comoving distance at epoch η to angle on the sky. It is given by

$$R_\eta(z)=\frac{2}{\Omega_0^2H_0(1+z)}\times\{\Omega_0z+(\Omega_0-2)[(1+\Omega_0z)^{1/2}-1]\}\ , \tag{33}$$

or equivalently,

$$R_\eta(\eta)=\begin{cases}\eta_0-\eta, & \Omega_0=1\ ,\\ \mathcal{R}\sinh[(\eta_0-\eta)/\mathcal{R}], & \Omega_0<1\ .\end{cases} \tag{34}$$

Efstathiou [6] takes the asymptotic form of Eq. (34) for $\eta_0\gg\eta$ [or $(\Omega_0z)^{1/2}\gg1$]. This is not a good approximation for $\Omega_0<1$ models in which the surface of last scattering was relatively recent. For example, if $\Omega_0=0.2$ and $h=0.8$, then $z_*\simeq20$.

For Compton-y distortions, the mean squared temperature fluctuation in principle has contributions from a uniform background y distortion, estimated by Eq. (17), as well as from fluctuations in the background. If no spectral information is obtained, it is not possible to observe the effects of the uniform distortion. However, in practice, given any realistic experimental window function, this is unlikely to be a concern; in small-scale experiments the uniform background is always subtracted out. For example, many experiments measure some algebraic combination of correlation functions

$$C(\theta,\sigma)=\left\langle\frac{\Delta T}{T}(\gamma_1)\frac{\Delta T}{T}(\gamma_2)\right\rangle_{\rm sky}\ , \tag{35}$$

where the average is performed with fixed beam throw $\theta=\arccos(\gamma_1\cdot\gamma_2)$ and with Gaussian beam width σ [$C(\theta,\sigma)$ is not to be confused with the Compton scattering collision terms $C(\mathbf{x},\mathbf{p})$]. The corresponding window function is given by

$$W_{\theta\phi}(q)=J_0(q\theta)\exp[-(q\sigma)^2]\ . \tag{36}$$

Actual experiments employ beam switching to minimize noise, e.g., a double beam experiment measures $(\Delta T/T)^2_{\rm double}=C(0,\sigma-C(\theta,\sigma)$. Whereas $C(\theta,\sigma)$ is sensitive to fluctuations from all scales greater than σ, $C(0,\sigma)-C(\theta,\sigma)$ is effectively only sensitive to angular scales between σ and θ, as one can see by examining Eq. (36). Even maps generated by interferometry are only sensitive to fluctuations below the size of the primary beam θ_{pb}.

The cancellation arguments, which say that $|\Delta(k,\mu,\eta)|$ is sharply peaked at $\mu=0$, allow us to set $\mu=0$ in the slowly varying terms, so that

$$\left[\frac{\Delta T}{T}\right]^2=\int_0^\infty Q(k)W(kR_\eta)dk/k\ , \tag{37}$$

where

$$Q(k)=\frac{K^2V_x k^3}{64\pi^2}\int_{-1}^{1}|\Delta(k,\mu,\eta)|^2 d\mu \tag{38}$$

expresses the power per logarithmic interval of the fluctuations.

Note that technically speaking since the square of the brightness distortion enters into (38), we need to worry about cross terms between first- and *third*-order processes. However, they are suppressed for two reasons. First, we are only interested in second-order effects when the first-order term is suppressed. The cross terms are thereby also suppressed. Second, as we shall see in Sec. III C, for the linear Doppler effect, the third-order terms that couple with the first-order term are also themselves suppressed. We will denote the order of the term by superscripts. For example,

$$\begin{aligned}\Delta&=\Delta^{(1)}+\Delta^{(2)}+\cdots\ ,\\ \delta&=\delta^{(1)}+\delta^{(2)}+\cdots\ ,\\ \mathbf{v}&=\mathbf{v}^{(1)}+\mathbf{v}^{(2)}+\cdots\ ,\end{aligned} \tag{39}$$

where superscript (1) refers to the values given by linear theory and (2) refers to the mildly nonlinear next order correction, etc.

Finally, it should be mentioned that Eq. (32) is only strictly valid for a thin last scattering surface. It assumes that there is a one-to-one correspondence between angles and length scales at last scattering given by Eq. (34). It also assumes that the phases of neighboring modes have been correlated by the scattering. We expect errors from these approximations to be of order $\delta\eta/(\eta_0-\eta_*)\simeq\eta_*/\eta_0$ ($\lesssim 0.2$ for realistic reionization scenarios).

C. Geometrical considerations

The physical picture becomes much clearer if we examine the geometrical aspects of the linear Doppler effects. Evolution under the linear Doppler and isotropic source terms can be expressed as

$$\dot{\Delta}+\gamma_i\partial_i\Delta+\dot{\tau}(\eta)\Delta=\dot{\tau}(\eta)[\Delta_0+\tfrac{1}{2}\Delta_2 P_2(\mu)+4\boldsymbol{\gamma}\cdot\mathbf{j}(\mathbf{x})]\ , \tag{40}$$

where

$$\mathbf{j}(\mathbf{x})=[1+\delta(\mathbf{x})]\mathbf{v}(\mathbf{x})=\mathbf{v}^{(1)}+\delta^{(1)}\mathbf{v}^{(1)}+\mathbf{v}^{(2)}+\cdots \tag{41}$$

is the so-called normalized matter current introduced by Vishniac [5]. As discussed in Sec. III A, $\Delta(k)\ll v(k)\ll\delta(k)$ at small scales. It will be demonstrated that for CDM and BDM power spectra, the mode coupling arises from a small enough scale that this condition is always satisfied. We have therefore dropped the second-order terms involving the anisotropy.

We can reinterpret Eq. (40) as representing scattering off a uniformly dense medium of electrons with velocity $\mathbf{j}(\mathbf{x})$. The increase in probability of scattering off overdense regions is then accounted for by a rescaling of the velocity field.

For the linear Doppler terms, we can also think of the cancellation argument [see discussion following Eq. (30)] as follows. If the matter current has zero vorticity, the contribution to the brightness fluctuation is approximately the line integral of the gradient of a field. The contribution is thus canceled apart from contributions from the end points. This is equivalent to the cancellation argument: if $\nabla\times\mathbf{j}(\mathbf{x})=\mathbf{0}$ then $\mathbf{j}(\mathbf{k})\|\mathbf{k}$ and thus $S(k,\mu,\eta)\propto\mu\simeq 0$.

Now let us consider the matter current vorticity: $\nabla\times\mathbf{j}(\mathbf{x})=[1+\delta(\mathbf{x})][\nabla\times\mathbf{v}(\mathbf{x})]-\mathbf{v}(\mathbf{x})\times\nabla\delta(\mathbf{x})$. Since gravitational perturbations of a pressureless fluid are irrotational, $\nabla\times\mathbf{v}(\mathbf{x})=\mathbf{0}$ to all orders. However, this is not true of the second term. The vorticity of the $(v\delta)$ term (and in second-order theory this term alone) does not vanish. Although the velocity field is the gradient of a potential, it is not the gradient of the local density field. Small-scale overdensities can move coherently with some peculiar motion along the line of sight. In these regions, there is an increased probability of scattering and inducing a Doppler shift in the background radiation temperature. This will imprint an anisotropy on the CMB at the scale of the scattering blobs. Note that this is an inherently nonlinear process since we are coupling a large scale (the scale of the velocity field) with a small scale (the scale of the overdensity). Recall that the Fourier transform of a product is a convolution, and

$$\mathbf{j}_{v\delta}(\mathbf{k})=\mathbf{v}*\delta=\int_0^\infty d^3k'\mathbf{v}(\mathbf{k}')\delta(\mathbf{k}-\mathbf{k}')\ ,$$

which shows the mode coupling explicitly. Since $\mathbf{v}(\mathbf{k}')\|\mathbf{k}'$, this gives a net nonzero contribution perpendicular to $\mathbf{k}$. In other words, we can have plane waves of the vector field $\mathbf{j}(\mathbf{x})$, with wave vector perpendicular to the line of sight, but with components parallel to the line of sight. This is exactly as required above: there is no cancellation between crests and troughs for the mode $\mathbf{k}\perp\boldsymbol{\gamma}$, but the Doppler effect does not vanish since $\boldsymbol{\gamma}\cdot\mathbf{j}\neq 0$.

It is also useful to note that the perpendicular and parallel components add in quadrature, i.e., the cross terms between the Vishniac term and other second-order terms cancel when we calculate $|\Delta(k,\mu,\eta)|^2$, as we now show. In all cases of interest, the source terms can be separated into a term dependent on conformal time and terms dependent on the mode coupling:

$$\begin{aligned}\eta_* g(\eta,\eta')S(\mathbf{k},\boldsymbol{\gamma},\eta')=\ & A(k\eta_*)G(r\equiv\eta'/\eta_*,\eta)\\ &\times\sum_{\mathbf{k}'}[F(\boldsymbol{\gamma},\mathbf{k},\mathbf{k}')\delta^{(1)}(\mathbf{k}',\eta_*)\\ &\times\delta^{(1)}(\mathbf{k}-\mathbf{k}',\eta_*)]\ ,\end{aligned} \tag{42}$$

where we have written the conformal time ratio η'/η_* as r. Therefore employing Eq. (26), we obtain the solution

$$\Delta^{(2)}(\mathbf{k},\gamma,\eta)\simeq A(k\eta_*)G(k\mu\eta_*)\times\exp(-ik\mu\eta)\left[\sum_{\mathbf{k}'}F(\gamma,\mathbf{k},\mathbf{k}')\delta^{(1)}(\mathbf{k}',\eta_*)\times\delta^{(1)}(\mathbf{k}-\mathbf{k}',\eta_*)\right], \tag{43}$$

where we have approximated the integral over conformal time as a Fourier transform by taking $\eta\to\infty$ in both the limits of the integral and in G: i.e.,

$$\int_0^\eta G(r,\eta)\exp(ik\mu\eta_* r)dr \simeq \int_0^\infty G(r,\eta=\infty)\exp(ik\mu\eta_* r)dr \simeq G(k\mu\eta_*)\ . \tag{44}$$

Hence $G(k\mu\eta_*)$ is the Fourier transform of $G(r,\eta=\infty)$ with $r\equiv\eta'/\eta_*$ as the Fourier conjugate of $k\mu\eta_*$. Note that the quadratic Doppler term also obeys Eq. (43) as we shall see in Sec. III F. On the other hand, the linear Doppler terms have the additional property that $F(\gamma,\mathbf{k},\mathbf{k}')=\gamma\cdot\mathbf{D}(\mathbf{k},\mathbf{k}')$ with $\mathbf{D}(\mathbf{k},\mathbf{k}')$ only a vector function of $\mathbf{k}$ and $\mathbf{k}'$. Choosing our coordinate system so that $\mathbf{k}\|\hat{\mathbf{x}}_3$ and γ lies in the x_1-x_2 plane, we can rewrite

$$F(\gamma,\mathbf{k},\mathbf{k}')=a_\parallel^{(2)}(k,k',\cos\theta)\gamma\cdot\mathbf{k}+a_\perp^{(2)}(k,k',\cos\theta)\gamma\cdot\mathbf{k}'_\perp = a_\parallel^{(2)}(k,k',\cos\theta)k\mu + a_\perp^{(2)}(k,k',\cos\theta)(1-\mu^2)^{1/2}k'\sin\theta\cos\phi\ , \tag{45}$$

where $\mathbf{k}'_\perp=k'(\sin\theta\cos\phi,\sin\theta\sin\phi,0)$ is the component of $\mathbf{k}'$ perpendicular to $\mathbf{k}$, and $a_\parallel^{(2)},a_\perp^{(2)}$ are arbitrary functions independent of the azimuthal angle ϕ. Thus we can separate the contributions into $\Delta^{(2)}=\Delta_\parallel^{(2)}+\Delta_\perp^{(2)}$ which are due to $\mathbf{j}\|\mathbf{k}$ and $\mathbf{j}\perp\mathbf{k}$.

Cross terms such as

$$\Delta_\parallel^{*(2)}\Delta_\perp^{(2)}\propto F_\parallel^*(\gamma,\mathbf{k},\mathbf{k}')F_\perp(\gamma,\mathbf{k},\mathbf{k}')|\delta^{(1)}(\mathbf{k}',\eta_*)|^2|\delta^{(1)}(\mathbf{k}-\mathbf{k}',\eta_*)|^2k'^2dk'\sin\theta\,d\theta\,d\phi \propto\int_0^{2\pi}\cos\phi\,d\phi=0 \tag{46}$$

then vanish under integration over the azimuthal angle ϕ. Here we have used the random phase hypothesis to eliminate one of the sums over modes. Of course, cross terms between first and second order vanish under this assumption as well.

Now consider the mixed first- and third-order term. This can be expressed as

$$\Delta^{*(1)}\Delta^{(3)}\propto\int_0^{2\pi}[a_\parallel^{(3)}(k,k',\cos\theta)k\mu+a_\perp^{(3)}(k,k',\cos\theta)(1-\mu^2)^{1/2}k'\sin\theta\cos\phi]d\phi\ . \tag{47}$$

The perpendicular part vanishes under the integration over azimuthal angle. However, the parallel part (for the linear Doppler effect) is suppressed, as we can see, by the additional factor of μ in Eq. (47). Hence mixed first- and third-order terms are not only suppressed by the smallness of the first-order term but also by a corresponding suppression in the third-order portion. These contributions are thus entirely negligible.

Since all relevant contributions add in quadrature, we can calculate them independently. In Sec. III D, we will calculate the first-order Doppler and isotropic effects; in Sec. III E, the Vishniac effect; and in Sec. III F the quadratic Doppler effect.

D. First-order Doppler and isotropic effects

In Fourier transform space, the solution to the residual first-order effect is given by

$$\Delta^{(1)}(\mathbf{k},\mu,\eta)=\int_0^\eta\left[\Delta_0^{(1)}+\frac{1}{2}P_2(\mu)\Delta_2^{(1)}+4\mu v^{(1)}\right]g(\eta,\eta')\exp[ik\mu(\eta'-\eta)]d\eta'\ . \tag{48}$$

Here we have retained the Δ contributions to the source in the first-order integral despite the suppression discussed in Sec. III B, since there is a corresponding suppression of the first-order linear Doppler source term that makes these two comparable. Note furthermore that for the first-order effect the source term is only a function of $\gamma\cdot\mathbf{k}=k\mu$ and not of γ in general.

Taking the zeroth moment with respect to μ of Eq. (48), we obtain

$$\Delta_0^{(1)}(\mathbf{k},\eta)=\int_0^\eta d\eta' g(\eta,\eta')\{\Delta_0^{(1)}j_0[k(\eta-\eta')]-4iv^{(1)}j_1[k(\eta-\eta')]-\tfrac{1}{2}\Delta_2^{(1)}j_2[k(\eta-\eta')]\}\ , \tag{49}$$

where we have employed the identity

$$j_n(z)=\tfrac{1}{2}(-i)^n\int_{-1}^1\exp(i\mu z)P_n(\mu)d\mu\ . \tag{50}$$

Because of the oscillation of the spherical Bessel functions, in each case the integral only has strong contributions around $k(\eta-\eta')\lesssim 1$. Since $k\eta_*\gg 1$, this implies $\eta\simeq\eta'$ (and of course, this is just the cancellation argument in a different guise). Therefore we can take the slowly varying quantities g, $\Delta_0^{(1)}$, and $v^{(1)}$ out of the integral. As we have discussed in Sec. III B, the first term

and third term are suppressed by a factor of order the optical depth across one wavelength of the perturbation. We can perform the integration over the second term in Eq. (48) by noting

$$\int_0^\infty j_n(z)dz = \frac{\pi^{1/2}}{2}\frac{\Gamma[\frac{1}{2}(n+1)]}{\Gamma[\frac{1}{2}(n+2)]} , \tag{51}$$

and therefore

$$\Delta_0^{(1)}(\mathbf{k},\eta) \simeq -\frac{4iv^{(1)}(\mathbf{k},\eta)}{k}\dot{\tau}(\eta) . \tag{52}$$

Taking the second moment of Eq. (48), ignoring the Δ terms, and extracting the slowly varying quantities, we obtain

$$\Delta_2^{(1)}(\mathbf{k},\eta) \simeq 4iv^{(1)}(\mathbf{k},\eta)\dot{\tau}(\eta) \times \int_0^\eta d\eta' \{ \tfrac{3}{5} j_3[k(\eta-\eta')] - \tfrac{2}{5} j_1[k(\eta-\eta')] \} . \tag{53}$$

However, employing Eq. (51), we see that $\Delta_2^{(1)}$ vanishes. The quadrupole term can thus be neglected as compared with the other sources.

Let us briefly discuss this somewhat counterintuitive result. Equation (52) tells us that the first-order Doppler effect can lead to a small isotropic fluctuation in the local brightness even though the fluctuation produced immediately after scattering is dipole in nature.

Consider the following idealized case: initially isotropic photons scatter off electrons in a plane wave velocity field with wave vector perpendicular to the line of sight. At a given zero crossing of the wave, there will be photons that arrive after scattering off a trough, and photons that arrive from the *opposite* direction having scattered off a peak. Both of these photons will carry the same energy shift and the directionally averaged brightness fluctuation will *not* vanish. Of course, this effect is not cumulative. After the photons have traveled another half wavelength, the average brightness fluctuation at this same zero crossing will be of opposite sign. This is the cancellation argument specialized for the present case: all but the most recent scattering will cancel. Equation (49) reflects this by providing strong contributions to the directionally averaged brightness perturbation only if $\eta \simeq \eta'$.

However, there actually is a secondary cumulative effect. Notice that from the original scattering the $\mu=0$ mode which escapes cancellation has zero fluctuation in first-order theory. However, at the zero crossing, scattering off the stationary electrons takes the perturbed photons from the $\mu \simeq \pm 1$ modes and populates the $\mu=0$ mode. These photons travel parallel to the line of sight. Furthermore, now all the brightness fluctuations are additive along the line of sight, and one observes a perturbation in brightness on the same scale as the velocity field. In this way, the isotropic term can contribute significantly.

The isotropic term is in practice of the same order of magnitude as the residual first-order term which arises because of the growth of perturbations during the transit time of the photon across the perturbation [13]. Let us separate the time dependence of the perturbations. If we express the growth of density perturbations in linear theory by

$$\delta^{(1)}(\mathbf{k},\eta) = \mathcal{D}(\eta,\eta_*)\delta^{(1)}(\mathbf{k},\eta^*) , \tag{54}$$

then the growth of velocity perturbations is

$$v^{(1)}(\mathbf{k},\eta) = i\frac{\mathbf{k}}{k^2}\left[\frac{d}{d\eta}\mathcal{D}(\eta,\eta_*)\right]\delta^{(1)}(\mathbf{k},\eta_*) , \tag{55}$$

where $\mathcal{D}(\eta,\eta_*) = D(\eta)/D(\eta_*)$ is the ratio of the growth factors [26]:

$$D(\eta) \propto \begin{cases} \eta^2, & \Omega_0 = 1 , \\ 3\sinh(\eta/\mathcal{R})[\sinh(\eta/\mathcal{R}) - (\eta/\mathcal{R})]/[\cosh(\eta/\mathcal{R})-1]^2 - 2, & \Omega_0 < 1 . \end{cases} \tag{56}$$

Hence, for $\Omega_0 = 1$ or $\eta/\mathcal{R} \ll 1$ [alternatively $(\Omega_0 z)^{1/2} \gg 1$], $\mathcal{D}(\eta,\eta_*) = (\eta/\eta_*)^2$. Efstathion [6] employs this approximation for $\Omega_0 < 1$ models. Again this is not a good approximation because of the fact that last scattering is so recent in these models. We use the correct growth factors here. Equation (48) can then be written as

$$\Delta^{(1)}(\mathbf{k},\mu,\eta) = \frac{8\delta^{(1)}(\mathbf{k},\eta_*)}{(k\eta_*)^2} e^{-ik\mu\eta} \int_0^\eta \frac{\eta_*^2}{2}\left[\frac{d}{d\eta'}\mathcal{D}(\eta',\eta_*)\right][\dot{\tau}(\eta') + ik\mu]g(\eta,\eta')e^{ik\mu\eta'}d\eta' . \tag{57}$$

The two optical depth factors in the isotropic contribution reflect the nature of this double scattering effect. Let us check that this solution is consistent with the assumption of small $\Delta_2^{(1)}$. Taking the second moment of Eq. (57) and employing (50), we obtain

$$\Delta_2^{(1)}(\mathbf{k},\eta) = \frac{8\delta^{(1)}(\mathbf{k},\eta_*)}{(k\eta_*)^2}\frac{\pi}{4k} \times \frac{d}{d\eta}\left\{\frac{\eta_*^2}{2}\left[\frac{d}{d\eta}\mathcal{D}(\eta,\eta_*)\right]\dot{\tau}(\eta)\right\} . \tag{58}$$

We see that $\Delta_2^{(1)}/\Delta_0^{(1)} \simeq O(1/k\eta_*) \ll 1$ and $\Delta_2^{(1)}$ is indeed small compared with the other source terms.

The integral over the conformal time in Eq. (57) is again approximately a Fourier transform [13] of

$$G_v(r,\eta) = \frac{1}{2}\left[\frac{d}{dr}\mathcal{D}(r\eta_*,\eta_*)\right]\dot{\tau}(r\eta_*)g(\eta,r\eta_*)\eta_*^2 - \frac{d}{dr}\left\{\frac{1}{2}\left[\frac{d}{dr}\mathcal{D}(r\eta_*,\eta_*)\right]g(\eta,r\eta_*)\eta_*\right\} , \tag{59}$$

where the transform is defined in Eq. (44). Hence

$$|\Delta^{(1)}(k,\mu,\eta)|^2=\frac{64P(k,\eta_*)}{(k\eta_*)^4}|G_v(k\mu\eta_*)|^2 , \quad (60)$$

where we have implicitly used the ergodic and random phase hypotheses. The power per logarithmic interval $Q(k)$ for the first-order Doppler effect is therefore

$$Q_v(k)=\frac{2}{\pi}\frac{V_x}{\eta_*^3}\frac{I_{\eta,v}}{(k\eta_*)^2}P(k,\eta_*) , \quad (61)$$

where

$$I_{\eta,v}\equiv\frac{1}{2\pi}\int_{-k\eta_*}^{k\eta_*}|G_v(k\mu\eta_*)|^2 d(k\mu\eta_*) \simeq\int_0^{\eta_0/\eta_*}|G_v(r,\eta_0)|^2 dr , \quad (62)$$

and we have used Parseval's theorem to approximate $I_{\eta,v}$. For full ionization with $\Omega_0=1$ and $\eta_*\ll\eta_0$, $I_{\eta,v}\simeq 6.38$. Efstathiou [6] employs this value in cases where the approximation is not very good. We shall see in Sec. III F that this can lead to a significant correction.

One might worry about the appearance of η_* in the expression for $Q(k)$, since there is a certain arbitrariness in the definition of the epoch of last scattering, e.g., Efstathiou [6] picks $\tau(\eta_*)=1$, whereas we might equally well have chosen the peak of the visibility function. Nevertheless, inspection of the growth factors in $P(k,\eta_*)$ and I_η shows that all dependence on η_* vanishes, as it must, since it has only been introduced as a convenient normalization epoch.

E. The Vishniac effect

Contributions to the brightness fluctuation due to the Vishniac term $S_{v\delta}(\mathbf{x},\gamma,\eta)=4\delta^{(1)}(\mathbf{x})[\gamma\cdot\mathbf{v}(\mathbf{x})]$ may be expressed as

$$\Delta^{(2)}_{v\delta}(k,\mu,\eta)=A_{v\delta}(k\eta_*)G_{v\delta}(k\mu\eta_*)\exp(-ik\mu\eta) \times\sum_{\mathbf{k}'}F_{v\delta}(\gamma,\mathbf{k},\mathbf{k}')\delta^{(1)}(\mathbf{k}',\eta_*)\delta^{(1)}(\mathbf{k}-\mathbf{k}',\eta_*) , \quad (63)$$

where

$$A_{v\delta}(k\eta_*)=\frac{4i}{k\eta_*} ,$$

$$G_{v\delta}(r,\eta)=\frac{1}{2}\left[\frac{d}{dr}\mathcal{D}(r\eta_*,\eta_*)\right]\mathcal{D}(r\eta_*,\eta_*)g(\eta,r\eta_*)\eta_* ,$$

$$F_{v\delta}(\gamma,\mathbf{k},\mathbf{k}')=\gamma\cdot\left[\frac{\mathbf{k}'}{|\mathbf{k}'|^2}+\frac{\mathbf{k}-\mathbf{k}'}{|\mathbf{k}-\mathbf{k}'|^2}\right]k , \quad (64)$$

with $G_{v\delta}(k\mu\eta_*)$ defined from $G_{v\delta}(r,\eta)$ as in Eq. (44). The cancellation argument manifests itself here in that $G_{v\delta}(k\mu\eta_*)$ is approximately the Fourier transform of a wide bell-shaped function $G_{v\delta}(r,\eta_0)$. If $k\eta_*\gg 1$, this implies that only for $|\mu|\ll 1$ does $G_{v\delta}(k\mu\eta_*)$ have strong contributions. Therefore we can set $\gamma\perp\mathbf{k}$ for the other slowly varying functions of μ. We are thus calculating the perpendicular part $\Delta_1^{(2)}$ alone as the Vishniac term.

We find that

$$Q_{v\delta}(k)=\frac{1}{8\pi^3}\frac{V_x^2}{\eta_*^6}(k\eta_*)^3 I_{\eta,v\delta}I_{k,v\delta}(k)P^2(k,\eta_*) , \quad (65)$$

where $I_{\eta,v\delta}$ is defined as in (62) in the obvious manner and

$$I_{k,v\delta}(k)=\int_0^\infty dy\int_{-1}^1 d(\cos\theta)\frac{(1-\cos^2\theta)(1-2y\cos\theta)^2}{(1+y^2-2y\cos\theta)^2} \times\frac{P[k(1+y^2-2y\cos\theta)^{1/2},\eta_*]}{P(k,\eta_*)} \times\frac{P[ky,\eta_*]}{P[k,\eta_*]} . \quad (66)$$

For full ionization $I_{\eta,v\delta}\simeq 6.38$ when $\Omega_0=1$ and $\eta_*\ll\eta_0$. Again Efstathiou [6] uses this value for all cases. In the next section, we shall see what corrections are necessary for the general case.

Care must be taken when evaluating the mode coupling [Eq. (66)]. The integrand has a divergence on the boundary at $y=1$, $\cos\theta=1$. As described in Sec. IV A, a resonance occurs when the density field $\delta^{(1)}(\mathbf{k}')$ has a wavelength of $k\simeq k'$ (which implies $y\simeq 1$) and the velocity field is coherent: $|\mathbf{k}-\mathbf{k}'|\ll k$ (i.e., $\cos\theta\simeq 1$). Furthermore, since $\mathbf{k}\perp\gamma$ to avoid cancellation, $(\mathbf{k}-\mathbf{k}')\|\gamma$ and yields a strong Doppler contribution. The integral itself does not diverge however, since for reasonable power spectra, the power on the largest scales tends toward zero. Nonetheless, it complicates the integral, since we can have significant coupling between the largest and smallest scales. Thus even though for pure power laws $I_{k,v\delta}$ is independent of k, we expect that realistic power spectra will deviate from this prediction. This is especially true for steeply red power spectra, where the large-scale velocity field is determined far above the scale of interest (i.e., k) where the power spectrum is quite different. Figure 1 displays the magnitude of this effect as a func-

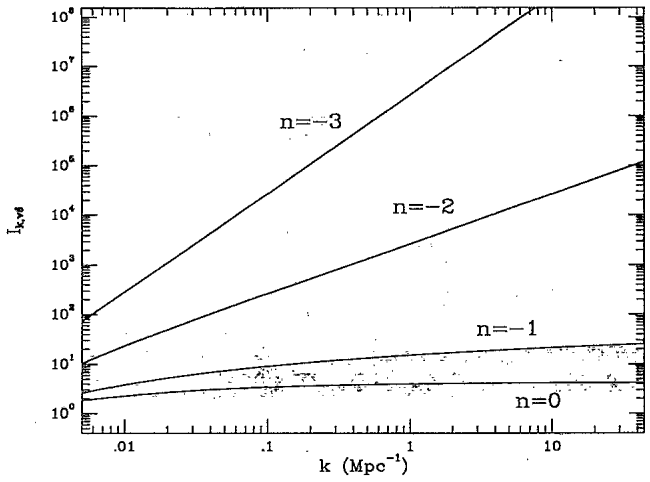

FIG. 1. Mode coupling integral for the Vishniac effect ($v\delta$) [see Eq. (66)] for various power laws [$P(k)\propto k^n$ for large k] with a large-scale cutoff at $k_{\min}=0.001$. Note that for steep power spectra the integral never approaches a constant. This represents a correction to the approximations in Ref. [6].

tion of k for various choices of the small-scale power law n and an arbitrary large-scale cutoff in power at $k_{\rm min}=0.001$ Mpc^{-1}. For reference the standard CDM model predicts $n=-3$, whereas BDM models prefer $n=-\frac{1}{2}$ but may plausibly lie in the range $0>n>-1$. This figure should only be taken heuristically since we have not included the proper large-scale behavior of a realistic power spectrum.

Now let us briefly consider the $O([\Delta-\Delta_0]\delta)$ term. As shown in Sec. III A, $\Delta(k)\lesssim v(k)$ for all k, so that the $O([\Delta-\Delta_0]\delta)$ term is smaller than the Vishniac term for *all* modes. An analysis of the Vishniac integral (66) for both CDM and BDM power spectra shows that it is dominated by modes well under the horizon for which $\Delta-\Delta_0\ll v$. The $O([\Delta-\Delta_0]\delta)$ term is thus completely negligible in these models.

F. The quadratic Doppler effect

The quadratic effect escapes cancellation since it is not directly proportional to $\boldsymbol{\gamma}\cdot\mathbf{k}=\mu$, but velocity perturbations are smaller than density perturbations at small scales, since in linear theory $v\propto\delta/k\eta$, if $\Omega_0=1$ or $(\Omega_0 z)^{1/2}\gg 1$. The effect is therefore relatively minimal at scales far below that of the horizon as long as the mode coupling is not significantly different from the Vishniac term.

The source term for the quadratic Doppler effect is

$$S_{vv}(\mathbf{x},\boldsymbol{\gamma},\eta)=-\mathbf{v}^{(1)}\cdot\mathbf{v}^{(1)}+7[\boldsymbol{\gamma}\cdot\mathbf{v}^{(1)}]^2 . \tag{67}$$

In Fourier space, a product becomes a convolution so that the solution can be written as

$$\Delta^{(2)}_{vv}(\mathbf{k},\boldsymbol{\gamma},\eta)=A_{vv}(k\eta_*)G_{vv}(k\mu\eta_*)\exp(-ik\mu\eta)\sum_{\mathbf{k}'}F_{vv}(\boldsymbol{\gamma},\mathbf{k},\mathbf{k}')\delta^{(1)}(\mathbf{k}',\eta_*)\delta^{(1)}(\mathbf{k}-\mathbf{k}',\eta_*) , \tag{68}$$

where

$$A_{vv}(k\eta_*)=\frac{4}{(k\eta_*)^2} ,$$

$$G_{vv}(r,\eta)=\left\{\frac{1}{2}\left[\frac{d}{dr}\mathcal{D}(r\eta_*,\eta_*)\right]\right\}^2 g(\eta,r\eta_*)\eta_* , \tag{69}$$

$$F_{vv}(\boldsymbol{\gamma},\mathbf{k},\mathbf{k}')=\frac{-\mathbf{k}'\cdot(\mathbf{k}-\mathbf{k}')+7(\boldsymbol{\gamma}\cdot\mathbf{k}')\boldsymbol{\gamma}\cdot(\mathbf{k}-\mathbf{k}')}{|\mathbf{k}-\mathbf{k}'|^2}\frac{k^2}{k'^2} .$$

Again $G(k\mu\eta_*)$ is approximately the Fourier transform of a wide bell-shaped function $G(r,\eta_0)$, and thus we can set $\boldsymbol{\gamma}\perp\mathbf{k}$ in the other terms. Notice that with this approximation

$$F_{vv}=-\frac{kk'\cos\theta+k'^2-7k'^2\sin^2\theta\cos^2\phi}{k^2+k'^2-2kk'\cos\theta}\frac{k^2}{k'^2} ,$$

so the cross terms between this term and the Vishniac term, $F_{v\delta}\propto\cos\phi$, vanish under integration over the azimuthal angle ϕ. Furthermore, the quadratic Doppler effect produces spectral distortions in addition to anisotropies so that in principle they can be isolated from the linear Doppler effect. In practice, however, we will find that the distortions from the quadratic Doppler effect are too small to be presently observable.

The solution is

$$Q_{vv}(k)=\frac{1}{\pi^3}\frac{V_x^2}{\eta_*^6}(k\eta_*)I_{\eta,vv}I_{k,vv}(k)P^2(k,\eta_*) , \tag{70}$$

where $I_{\eta,vv}$ is defined as in (62) and

$$I_{k,vv}=\int_0^\infty dy\int_{-1}^{+1}d(\cos\theta)\frac{(y-\cos\theta)^2-7(1-\cos^2\theta)(y-\cos\theta)y+(147/8)(1-\cos^2\theta)^2y^2}{(1+y^2-2y\cos\theta)^2}$$

$$\times\frac{P[k(1+y^2-2y\cos\theta)^{1/2},\eta_*]}{P[k,\eta_*]}\frac{P[ky,\eta_*]}{P[k,\eta_*]} . \tag{71}$$

We have inserted the $K=-2$ factor from (31) under the assumption that we are observing the Rayleigh-Jeans temperature distortions from this effect. For full ionization, $\Omega_0=1$, and $\eta_*\ll\eta_0$, we find $I_{\eta,vv}\simeq\frac{3}{2}$. In the general case, this value will be different, as will $I_{\eta,v}$ and $I_{\eta,v\delta}$. This is because I_η reflects the growth of perturbations as compared with their value at η_*, weighted by the probability of scattering at such an epoch. Perturbations grow more slowly in an open universe. If the integral is peaked above η_*, as is $I_{\eta,v\delta}$ and $I_{\eta,vv}$, the integral will decrease; if it is peaked below η_*, it will increase, as with $I_{\eta,v}$. There is also a small effect due to cutting off the integral at the present time η_0. Figure 2 shows the values of I_η as a function of Ω_B for $\Omega_0=\Omega_B$ and for $\Omega_0=1$.

Note that Eq. (71) is very similar to the Vishniac $I_{k,v\delta}$ integral. Therefore the k dependence of $Q(k)$ will resemble the Vishniac power spectrum save for the extra $1/(k\eta_*)^2$ term suppression at small scales. Thus, unless

$$\frac{I_{k,vv}}{I_{k,v\delta}}\gtrsim\frac{1}{8}(k\eta_*)^2\frac{I_{\eta,v\delta}}{I_{\eta,vv}} , \tag{72}$$

we expect the quadratic Doppler effect to be smaller than the Vishniac effect at small angular scales. We calculate this ratio explicitly for a range of power laws, again with

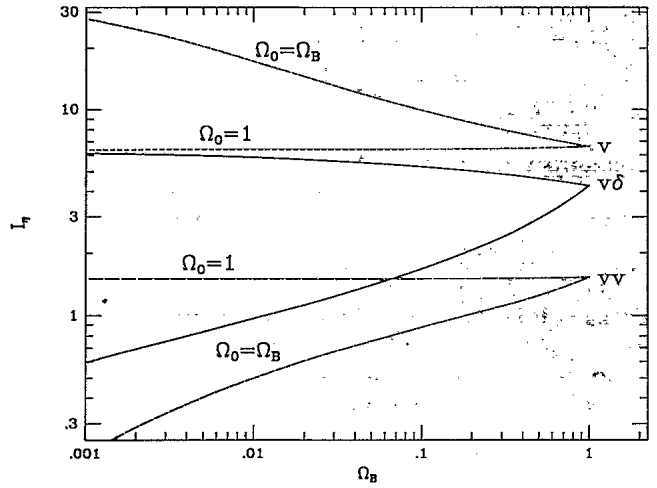

FIG. 2. The conformal time integrals I_η [see Eq. (62)] for the $O(v)$, $O(v\delta)$, and $O(vv)$ effects for various models. Note that for $\Omega_0 \ll 1$ the values depart significantly from the asymptotic $\Omega_0=1, \Omega_B \ll 1$ result. Again this significantly improves upon the approximations of Ref. [6].

an arbitrary large-scale cutoff in power at $k_{\min}=0.001$ Mpc^{-1} (see Fig. 3). In no case is the ratio sufficiently large to satisfy Eq. (72) for $k\eta_* \gg 1$. At scales nearer the horizon at last scattering, the linear first-order Doppler effect is not canceled, since there are only order 1 scattering blobs of this size across the last scattering surface. Therefore, the quadratic Doppler effect plays no significant role at these scales either. Note that this also implies that the $O([\Delta-\Delta_0]v)$ term is negligible as well.

IV. CALCULATIONS FOR SPECIFIC COSMOLOGICAL MODELS

A. Cold dark matter (CDM) scenario

Recent comparisons of anisotropy limits from the South Pole 1991 experiment [3], with CDM normalized to COBE, have suggested that some CDM models, especially those with high Ω_B, may be ruled out, e.g., [27,28]. One possible resolution is to have early reionization to at least partially erase the primordial anisotropies on degree scales. If this were the case, then secondary anisotropies would tend to be generated on smaller scales, which we now consider in detail.

The CDM power spectrum is given by [29]

$$P(k,\eta_0)=\frac{Ak}{\{1+[ak+(bk)^{3/2}+(ck)^2]^\nu\}^{2/\nu}}, \tag{73}$$

where $a=6.4(\Gamma h)^{-1}$ Mpc, $b=3.0(\Gamma h)^{-1}$ Mpc, $c=1.7(\Gamma h)^{-1}$ Mpc, and $\nu=1.13$. For standard CDM, $\Gamma=0.5$. The normalization constant A is given by COBE to be [29]

$$A=5.2\times10^5\left[\frac{Q_{\rm rms}}{16\mu K}\right]^2\frac{(h^{-1}\ {\rm Mpc})^4}{V_x}. \tag{74}$$

Figure 4 shows the radiation power spectrum $Q(k)$ for the various effects in a universe that never recombines: $x_e(z)=1$. For comparison, we have plotted the primordial fluctuations from standard recombination [30] in Fig. 4. As expected, first-order and quadratic Doppler terms are suppressed at small scales. Furthermore, the quadratic effect never dominates on any scale. The result for the correlation function is plotted in Fig. 5. Here the correlations are given for infinite beam resolution $\sigma=0$. Note that the coherence scale is somewhat under an arcminute.

To obtain observable quantities, the formulas of Wilson and Silk [31] can be employed, or we can note that for CDM on arcminute scales and greater, a double beam experiment essentially measures $C(0,\sigma)$, whereas a triple beam experiment measures $\frac{3}{2}\ C(0,\sigma)$ for the Vishniac effect, due to the small coherence scale. In Fig. 6, we show the predictions of $C(0,\sigma)$ for CDM with several values of Ω_B.

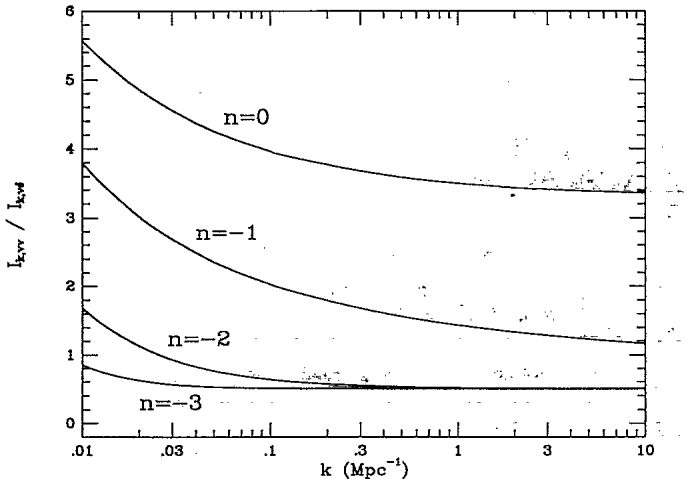

FIG. 3. Ratio of mode coupling integrals, i.e., I_k of the quadratic Doppler effect (vv) to that of the Vishniac effect ($v\delta$). For no power law does the ratio become sufficiently large to make the quadratic Doppler term significant compared with the Vishniac term, at small scales [see Eq. (72)].

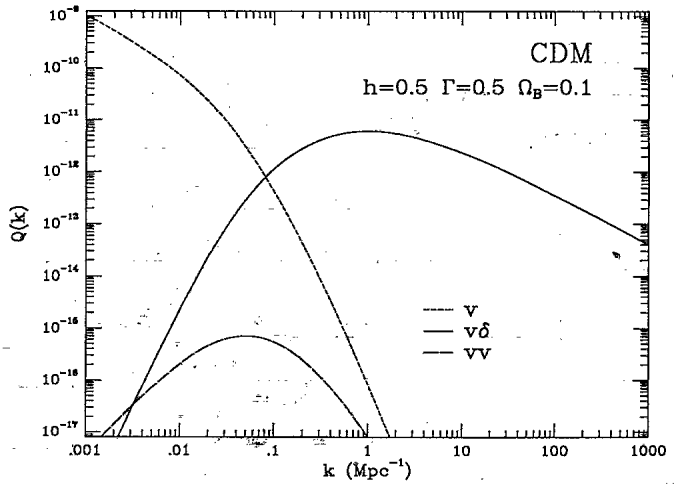

FIG. 4. CDM radiation fluctuation power spectrum for the first order Doppler (v), Vishniac ($v\delta$), and quadratic Doppler (vv) effects. Here $Q(k)$ is the power per logarithmic interval, i.e., $C(0)=\int Q(k)dk/k$. The shape parameter Γ [see Eq. (73)] is 0.5 for standard CDM. Note that the (vv) term is never significant: (v) dominates at large scales and ($v\delta$) dominates at small scales.

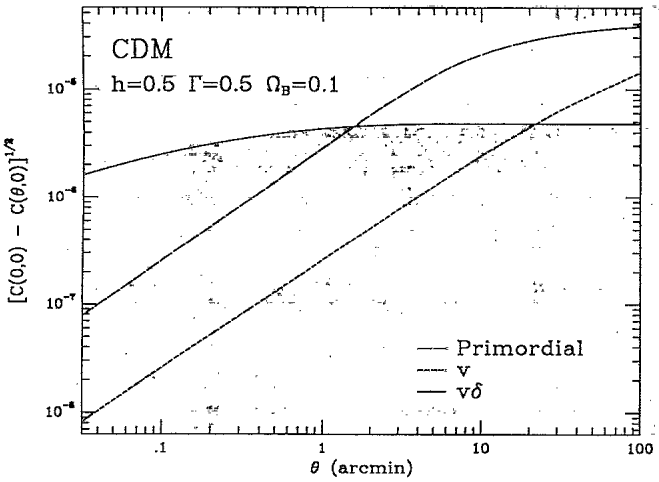

FIG. 5. CDM predictions for a double beam experiment with infinite resolution. The primordial fluctuations for standard recombination are normalized to COBE [2]. Note that at subarcminute scales the Vishniac ($v\delta$) term dominates over the first-order Doppler term (v) and can be larger than the primordial fluctuations. Also note that the coherence scale of the Vishniac effect for CDM is somewhat under an arcminute.

Recently, Tegmark and Silk [32] have shown that reionization may plausibly occur as early as $z_i \simeq 50$. Furthermore, they show that reionization is sudden in realistic models, so that $x_e(z)$ is essentially a step function at z_i. For these models, the optical depth will never reach unity until the standard epoch of recombination, and hence some primordial anisotropies remain. We will approximate this by employing the cumulative visibility function

$$g_C(\eta_i) = \int_{\eta_i}^{\eta_0} g(\eta_0, \eta') d\eta' , \tag{75}$$

which tells us the fraction of the CMB photons which have been rescattered since z_i and have thus suffered suppression of primordial fluctuations. In terms of the temperature fluctuations, only a fraction $f_{\rm prim}(\eta_i) = 1 - g_C(\eta_i)$ of the original signal remains after rescattering. We have checked this estimate against the numerical solutions in Sugiyama, Silk, and Vittorio [33] and found good agreement.

Of course, the Vishniac effect decreases if the optical depth never reduces unity on the new last scattering surface. In this case, the epoch of new last scattering η_* is not the conformal time when optical depth reaches unity. We can, however, characterize this epoch by the maximum of the visibility function. Employing this definition, we can express the fraction of the full effect for these models as $f^2_{v\delta}(\eta_i) = \mathcal{Q}_{v\delta}/\mathcal{Q}_{v\delta}|_{\tau(\eta_*)=1}$. Figure 7 plots the weighting fraction $f(\eta_i)$ for the Vishniac effect and the primordial fluctuations. Notice that these fractions are dependent only on the cosmological parameters Ω_0, Ω_B, h and not on the power spectrum of a given model. This fraction squared should be multiplied by the values in Fig. 4 to obtain the radiation power spectrum in cases when optical depth never reaches unity on the new surface of last scattering. Notice that we still obtain a fairly large Vishniac effect even when only a fraction of photons have scattered and the primordial fluctuations are only partially reduced. For example, if $\Omega_B = 0.1$ and $z_i \simeq 20$ then $f_{\rm prim} \simeq f_{v\delta} \simeq 0.83$, i.e., 83% of the primordial fluctuations remain whereas 83% of the fluctuations from the Vishniac effect are generated. This is because the Vishniac effect becomes stronger at later times due to the growth of the velocities. Therefore, even though only a small fraction of photons are rescattered, a relatively large anisotropy is imprinted on them. So late reionization will *not* yield smaller CMB fluctuations on the arcminute level.

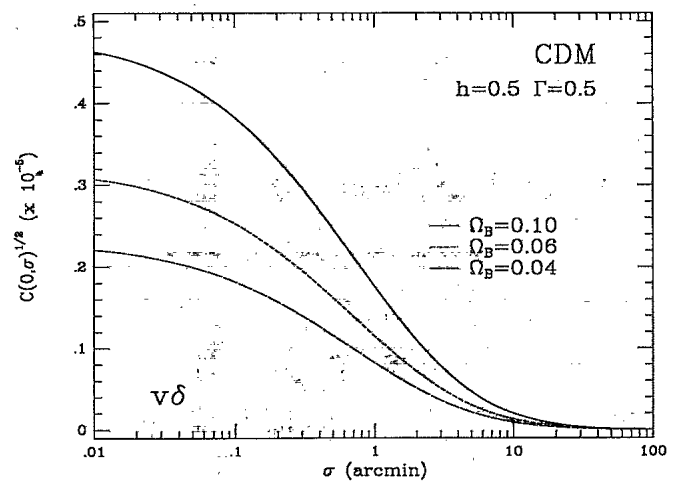

FIG. 6. CDM predictions of the Vishniac effect for $C(0,\sigma)$ with various choices of Ω_B. Because the coherence scale is under an arcminute, experiments at arcminute scales and greater will essentially only measure $C(0,\sigma)$.

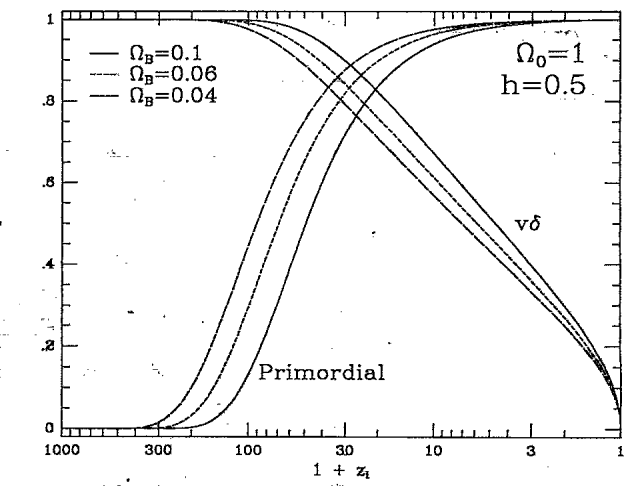

FIG. 7. Weighting fraction for models with sudden reionization at z_i in a flat $\Omega_0 = 1$ universe. For example, in the CDM model, the full values of Fig. 4 should be weighted by f^2 to determine fluctuations for these ionization histories. Notice that we still obtain a strong Vishniac effect even in cases where the primordial fluctuations are only partially erased. At $z_i \simeq 20$, we have approximately 83% of both the Vishniac and primordial fluctuations. Late reionization therefore does not necessarily yield smaller fluctuations.

TABLE I. Predictions of $C(0,\sigma)$ ($\times 10^{-5}$) for the Vishniac effect for various models which can be tested by future experiments at the VLA, ATCA, and OVRO. We have chosen three representative values of the beam smoothing σ. ATCA and OVRO have similar effective beam smoothing. Ranges given in the sixth and seventh columns represent the uncertainty in predictions due to nonlinearity. The observed signal will also depend on the first-order effect which in turn depends sensitively on the nature of the experiment and not on $C(0,\sigma)$ alone.

Model	Ω_B	h	Spectrum	x_e	$\sigma=0.1$ arc min	$\sigma=0.5'$	$\sigma=1.0'$
BDM	0.2	0.8	$n=0$	1.0	2.61–11.50	1.17–1.19	0.48
BDM	0.1	0.8	$n=-0.5$	1.0	2.17–3.26	0.80	0.48
BDM	0.1	0.5	$n=-0.5$	1.0	1.77–2.36	0.49	0.25
BDM	0.2	0.8	$n=0$	0.1	1.23–1.35	0.13	0.05
BDM	0.2	0.8	$n=-0.5$	0.1	0.83	0.18	0.09
CDM	0.1	0.5	$\Gamma=0.5$	1.0	0.38	0.25	0.18
CDM	0.1	0.5	$\Gamma=0.2$	1.0	0.04	0.03	0.03

We have also tested a phenomenologically successful model inspired by CDM that sets $\Gamma=0.2$. This has the effect of suppressing the small-scale power with respect to the large leading to an extremely small Vishniac effect (see Table I).

B. Baryonic dark matter (BDM) scenario

Baryonic dark matter models with isocurvature fluctuations contain relatively large amounts of small-scale power (for the power spectrum in these models, see [34,35]). For this reason, primordial fluctuations from the first-order Doppler effect at standard recombination are overproduced on the scale of the comoving particle horizon (i.e., η). The angle subtended by the horizon at redshift z is

$$2\sin(\theta_H/2)=\frac{\Omega_0(\Omega_0 z+1)^{1/2}}{\Omega_0 z+(\Omega_0-2)[(\Omega_0 z+1)^{1/2}-1]} \quad (76)$$

At standard recombination $z\simeq 1100$ and $\theta_H\simeq 1°$. Reionization is therefore necessary to remove these degree scale fluctuations. Generally, anisotropies will be erased up to the scale of the horizon size at the epoch z_* where the optical depth reaches unity. Secondary fluctuations from the first-order Doppler effect on the new last scattering surface will of course be generated, and will peak near the horizon size at z_*. Since the horizon scale is then larger than at standard recombination, the degree scale constraints on CMB fluctuations can be avoided. Primary fluctuations on degree scales will be erased and secondary fluctuations will be smaller because they have lower amplitude *and* because degree scales are well below their peak.

In Fig. 8, we plot the angle subtended by the horizon at $\tau(\eta_*)=1$ for $h=0.8$. Notice that if $\Omega_0=0.1$–0.2 as suggested by some dynamical measurements, the horizon at last scattering subtends $\sim 15°$ today. Therefore at degree scales, there is significant cancellation as described above. However, for the case in which the total density includes matter that does not contribute to the free electron density in the intergalactic medium (IGM), i.e., if baryons are hidden in compact objects or the ionization fraction is less than unity, then the last scattering surface is further away. In low Ω_0 universes, the angle subtended by the horizon at last scattering is only marginally larger than that at standard recombination. These models are therefore in danger of producing secondary fluctuations on degree scales which are as large as the primordial ones that have been erased.

The relatively high amount of small-scale power in these models also leads to large (and in fact observable) fluctuations at arcminute scales due to the Vishniac effect. Thus even models with a relatively late last scattering epoch can be constrained. We normalize the spectrum to the fractional mass fluctuation on a scale of $8h^{-1}$ Mpc, i.e., $\sigma_8=1$. One complication arises, however. We have performed our calculations in linear theory and therefore can only realistically predict fluctuations on scales larger than the nonlinearity scale. We define the nonlinearity scale as the value k_{nl} for which

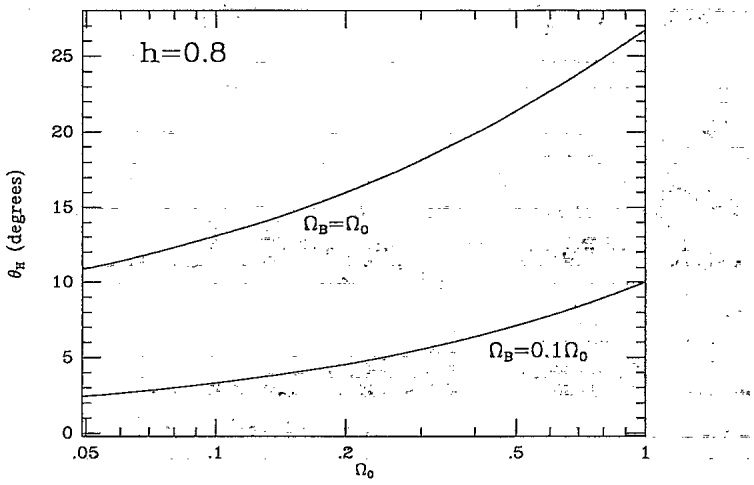

FIG. 8. Angle subtended by the horizon at last scattering (optical depth unity), i.e., η_* [see Eq. (76)], for $h=0.8$ in models with complete reionization, i.e., $x_e=1$. In models where $\Omega_B=\Omega_0$, the horizon size is sufficiently large to escape degree scale constraints. However, models which hide matter in compact objects or have low ionization fraction will have horizon sizes close to the degree scale. We have plotted for illustrative purposes a model in which 90% of the baryons are in compact objects ($\Omega_B=0.1\Omega_0$) or alternatively ionized fraction $x_e=0.1$.

$$\frac{V_x}{2\pi^2}\int_0^{k_{nl}} P(k,\eta_*)k^2dk = 1 \ , \tag{77}$$

corresponding to the scale on which $\delta\rho/\rho \simeq 1$. The maximum anisotropy comes from taking the linear power spectrum out to infinitely small scales. The minimum anisotropy we expect comes from cutting off fluctuations at scales smaller than the nonlinearity scale, i.e., setting $Q(k > k_{nl}) = 0$. Thus the true prediction lies somewhere between this minimum and maximum, the uncertainty being caused by our ignorance of nonlinear effects, although we would expect the prediction using the cutoff at k_{nl} to be more realistic. Choosing $\Omega_0 = 0.2$ and $h = 0.7$ as an example, we plot the results of using this prescription for various choices of the power law index n in Fig. 9. Note that for $n > -1.5$ the fluctuations due to the Vishniac effect increase with decreasing angular size, and therefore all experiments will effectively measure $C(0,\sigma)$.

Recent measurements from the Very Large Array (VLA) have yielded significant improvements in the constraints on arcsecond fluctuations in the CMB. Fomalont *et al.* [36] report $C(0,\sigma)^{1/2} \times 10^5 < 1.9, 2.1, 2.3, 4.0, 5.8, 7.2$ for $\sigma = 0.56, 0.40, 0.22, 0.15, 0.10$ arc min respectively. Unfortunately, due to the uncertainty about effects below the nonlinearity scale, the arcsecond measurements cannot be used to constrain most of the BDM models, and the larger angle measurements do not yet yield an improvement over the Owens Valley Radio Observatory (OVRO) [37] measurements at $\sigma = 0.78$ arc min. On the other hand, a small improvement in the measurements at $\sigma > 0.2$ arc min would rule out many favored models, e.g., $\Omega_0 = 0.2$, $h = 0.8$, $n = 0$, $x_e = 1$ (see Table I).

The most stringent constraints to date come from the Australian Telescope Compact Array (ATCA) which uses interferometry to make a sky map. They place an upper limit of $(\Delta T/T)_{\rm ATCA} < 0.9 \times 10^{-5}$ on an angular scale of $l \simeq 4500$ or equivalently 0.76 arc min [7]. However, care must be taken when interpreting this limit due to the peculiar nature of the ATCA window function. This window function is given by Eq. (8) and Fig. (6) of Ref. [7]. Note that the filter function depicted in their figure (6) has been arbitrarily normalized to peak at unity. In the definition of the window function appropriate for temperature fluctuations [see Eq. (32)], the peak value of the filter function is 0.52 [38]. This normalization is important for comparison to other experiments. For example, OVRO quotes an upper limit for temperature fluctuations with a window function appropriate for a triple beam experiment with $\theta = 7.15$ and $\sigma = 0.78$ arc min [37]:

$$\left[\frac{\Delta T}{T}\right]_{\rm OVRO} = \{2[C(0,\sigma) - C(\theta,\sigma)] - \tfrac{1}{2}[C(0,\sigma) - C(2\theta,\sigma)]\}^{1/2} < 2.1 \times 10^{-5} \ . \tag{78}$$

We plot the ATCA and OVRO window functions with their proper normalization in Fig. 10. The two window functions are similar in the range $kR_\eta \simeq l \gtrsim 4500$. Therefore, the upper limits are directly comparable for fluctuations on these scales. Since the upper limit of ATCA is a factor of 2 more stringent, ATCA places the strongest constraints for $l \gtrsim 4500$. However, OVRO is significantly more sensitive for $l \lesssim 4500$. Because the Vishniac effect peaks at small scales for $n > -1.5$, the ATCA experiment is the most sensitive probe of these secondary fluctuations. For effects that do not peak at the smallest angular scale, e.g., the first-order Doppler effect, the OVRO experiment will be more sensitive.

The ATCA and OVRO limits correspondingly place constraints on the BDM model parameters Ω_0 and n (see Fig. 11). We have included the first-order term Q_v, but

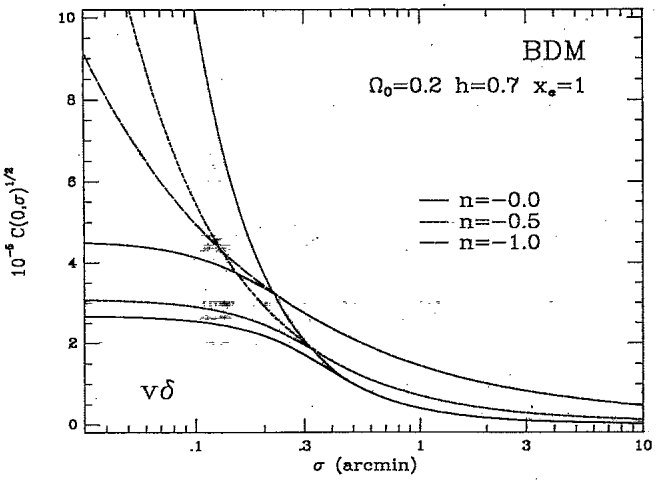

FIG. 9. BDM predictions for $C(0,\sigma)$ from the Vishniac effect with $\Omega_0 = 0.2, h = 0.7, x_e = 1.0$. Notice that at arcseconds, we are in the nonlinear regime; uncertainties here greatly inhibit our ability to constrain models. We have plotted predicted fluctuations with (heavy) and without (light) the cutoff at k_{nl}. These should be taken as lower and upper bounds for the predictions.

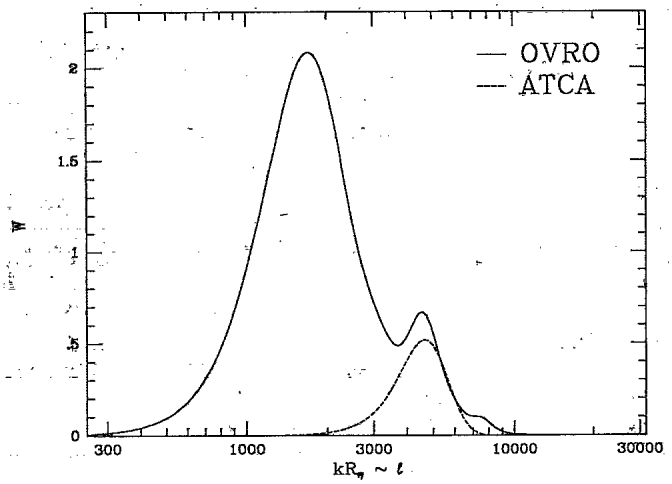

FIG. 10. The ATCA and OVRO window functions compared. Notice that the two window functions are comparable for $l \gtrsim 4500$. OVRO, however, is far more sensitive to fluctuations with $l \lesssim 4500$. We use the small-angle approximation: $kR_\eta \simeq l$.

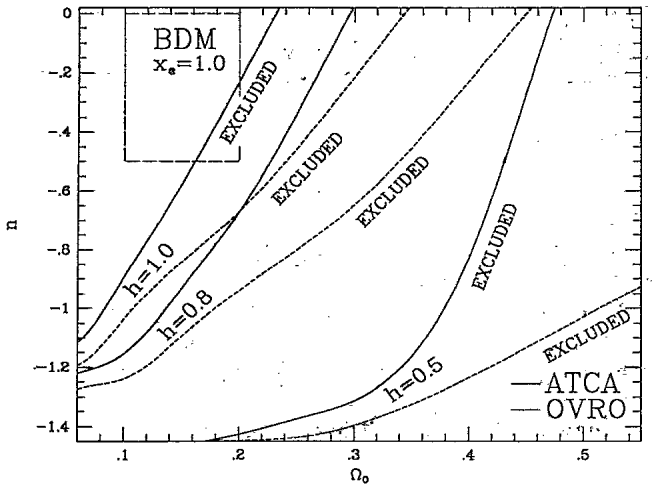

FIG. 11. The constraints on fully ionized (i.e., $x_e=1$) BDM models from the measurements of ATCA $(\Delta T/T)_{\rm ATCA} < 0.9\times10^{-5}$ (solid line) and OVRO $(\Delta T/T)_{\rm OVRO} < 2.1\times10^{-5}$ (short dashed line). The constraints are strong functions of the Hubble constant; here we show three representative values of h, the lowest and highest values generally considered and the specific value ($h=0.8$). This value and the region of Ω_0-n space enclosed by the box (long dashed line) represent the parameters chosen by Ref. [35]. Low n and high Ω_0 are excluded. Note that other assumptions about x_e would alter these limits.

given the scale and the width of the ATCA window function, the ATCA constraint essentially comes from the Vishniac term alone. The OVRO constraint has a small contribution from the first-order effect for steep values of n. Notice that for $n>-1.5$, ATCA constrains BDM models more stringently than OVRO. It might also be mentioned that the constraint is a sensitive function of the upper limit. An improvement in the upper limit of less than a factor of 2 would rule out the favored model of $\Omega_0=0.2$, $h=0.8$, $n=-0.5$, $x_e=1$ [35].

Our constraints differ from those of Efstathiou [6], even accounting for the new limits. In particular, his scaling relations cannot be extended to certain regions of parameter space. The correction for the angle to distance relation R_η [Eq. (34)] tends to increase the Vishniac effect for large n and decrease the first-order term for small n. The true conformal time integrals I_η (Fig. 2) tend to decrease the Vishniac term and increase the first-order term for low Ω_0. The net effect is an increase in the predictions for low Ω_0 and high n and a decrease in the predictions for low Ω_0 and low n. It is also interesting to note that the smaller scale experiments do a better job of constraining high n as opposed to low n. This is useful since the arcminute measurements tend to constrain low n (see Table I).

Such constraints could be avoided by changing the ionization history. In fact, some modification from the fully ionized scenario is also necessary to escape limits on the Compton-y parameter [21]. Excessive spectral distortions can be avoided by a relatively late ionization so that the optical depth during the reionization epoch, while greater than unity, does not reach large values. However, since anisotropies unlike spectral distortions come mostly from the last scattering event, the small angular scale constraints cannot be evaded in a similar manner. The secondary anisotropies are most sensitive to the location of the last scattering surface rather than the events that preceded it. An *ad hoc* way of moving the last scattering surface would be to lower the ionization fraction to a smaller constant value, e.g., $x_e=0.1$ [35], but it is difficult to see how the ionization fraction can be kept at a small but significant value since the recombination time tends to be short. In these models, the predictions of the Vishniac effect for the ATCA experiment are then below the observational limits (see Table I) for all interesting choices of the BDM parameters. On the other hand, an increase in the first-order term would appear in any of the larger angle experiments such as OVRO or, even more significantly, the degree scale experiments. This is because the last scattering surface becomes distant and cancellation incomplete. In general, whereas $O(v\delta)$ secondary anisotropies decrease with z_*, $O(v)$ anisotropies actually *increase* with z_*. If we decrease the ionization fraction substantially more than $x_e\simeq0.1$, although primordial anisotropies will be erased, new ones of roughly the same size will be generated. These models may therefore overproduce fluctuations on degree scales (see Fig. 8).

A more physically motivated way of avoiding the constraints would be to hide the baryons in black holes [21]. Obviously, this has an effect quite similar to lowering the ionization fraction. For simplicity let us assume that the matter power spectrum is unchanged from the $\Omega_B=\Omega_0$ case [recall that we have defined Ω_B as the fractional baryon density in the intergalactic medium (IGM)]. Figure 12 shows how the combined Vishniac and first-order anisotropies are changed in this case of $\Omega_B<\Omega_0$. We have plotted here the predictions for an experiment with a setup similar to OVRO ($\theta=7.15$, $\sigma=0.78$ arc min).

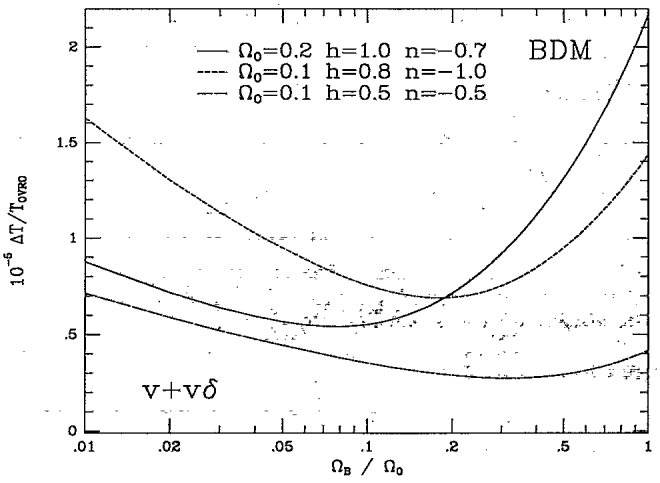

FIG. 12. Combined first-order and Vishniac predictions for the OVRO triple beam experiment ($\theta=7.15, \sigma=0.87$ arc min) from three representative BDM models with a significant fraction of the baryons in compact objects which do not contribute to the baryon density in the intergalactic medium, Ω_B. The first-order effect dominates for low Ω_B, since the last scattering surface is then at such high redshift.

The increase in fluctuations for $\Omega_B/\Omega_0 \ll 1$ is from the first-order term and, as described above, is quite significant. For models in which the last scattering surface would already have been distant (e.g., $\Omega_0=0.1$, $h=0.5$) the increase in the first-order term is strong enough so that lowering the number of baryons in the IGM actually increases the predicted fluctuations on arcminute scales. In most cases, hiding the baryons can only decrease the predictions by a factor of ~ 2. With modest future improvements in experiments, the isocurvature BDM model can be tested for all ionization histories.

V. CONCLUSIONS

We have shown that anisotropies on arcminute angular scales can provide a powerful probe of the ionization history of the Universe. The COBE DMR detection of large-angular scale anisotropies implies intermediate angular scale anisotropies (when combined with CDM or BDM power spectra) that, in the absence of reionization, exceed or are comparable to observational limits. Reionization is essential in BDM models, and *may be essential* in CDM models, e.g., [27,28]. Moreover, efficient reionization *must* have occurred at $z>5$. Reionization has sufficiently modest energetic requirements (at least for photoionization) that it plausibly occurred when only a small fraction of the Universe was found in nonlinear structures [32]. This occurs as early as $z \simeq 1000$ in BDM and $z \simeq 50$ in unbiased CDM models. While reionization helps suppress, or at least reduce, primordial fluctuations on degree scales due to the first-order Doppler effect at standard recombination, it inevitably regenerates secondary fluctuations on arcminute scales.

We have considered all Compton scattering effects to second order and have shown explicitly that only those of $O(v)$ and $O(v\delta)$ play a significant role in regeneration for realistic power spectra; i.e., no other higher-order effects are important, and there are no hidden terms to cancel the Vishniac term. However, for a (less realistic) power spectrum that peaks above the horizon scale at last scattering, the $O([\Delta-\Delta_0]\delta)$ term *can* significantly cancel the Vishniac effect. Furthermore, we have substantially improved the approximations involved in calculating these effects in an open universe. The $O(v^2)$ effect, although small, sets the minimal spectral (Compton-y) distortion in reionization scenarios. For the CDM model, all of these secondary effects predict fluctuations well below present observations. However, one should note that even in cases where the primordial fluctuations are not efficiently erased due to relatively late reionization, the Vishniac effect *still* generates fluctuations that are of the same order as primordial fluctuations at arcminute scales. For BDM models where early reionization is necessary, new measurements from ATCA already exclude a significant region of (Ω_0,n) parameter space. Changing the ionization history can avoid the present constraints, but it is difficult to decrease the secondary fluctuations by a significant amount. If one arranges the ionization history to produce a small Vishniac effect, the first-order Doppler effect will be correspondingly increased. We therefore find for both CDM and BDM that changing the ionization history through what might be considered physically well-motivated prescriptions does not in fact greatly change the predictions for the secondary anisotropies.

ACKNOWLEDGMENTS

We are indebted to Scott Dodelson for redirecting us toward properly evaluating the collision integral. We are grateful to Jim Peebles and Renyue Cen for providing their BDM power spectra. We acknowledge many useful discussions with Roman Juszkiewicz, Naoshi Sugiyama, Max Tegmark, and Martin White. We thank Ravi Subrahmanyan for detailed discussions of the ATCA experiment. D.S. was supported by the U.K. SERC/NATO and by the CfPA. W.H. was supported by the NSF. This work has been further supported in part by grants from NSF and DOE.

APPENDIX A: COLLISIONLESS BOLTZMANN EQUATION

Second-order gravitational effects play an important role when the first-order *gravitational* effect vanishes, e.g., if there are no metric fluctuations on the last scattering surface as in the case of late phase transition scenarios. These effects will primarily manifest themselves on large scales. Martinez-Gonzalez *et al.* [39] have performed the calculation for weakly nonlinear effects due to second-order density perturbations. Here we complete the program by deriving all possible effects to second order in the metric perturbations. Note, however, that recently Jaffe *et al.* [40] have shown that scenarios in which there are no fluctuations on the last scattering surface must involve strongly nonlinear effects to generate the observed gravitational potentials today. They find that such models must generate CMB fluctuations on the order of, or greater than, the standard primordial fluctuations. Therefore, even for this class of models, weakly nonlinear effects such as those derived here may only play the role of a small correction to the full gravitational effect.

We choose to work in the synchronous gauge, following closely the notation of Peebles and Yu [41]. In this gauge, perturbations to the metric are expressed as

$$g_{00}=1, \quad g_{0i}=0, \quad g_{ij}=-a(t)^2[\delta_{ij}-h_{ij}(x,t)] , \quad \text{(A1)}$$

where Greek indices run from 0 to 3 and Latin indices run from 1 to 3. Summation over repeated indices is assumed throughout even when all indices are lowered. The momentum of the photon will be denoted by p^μ and for convenience we express

$$p_i=-p_0 a(t) e \gamma_i , \quad \text{(A2)}$$

where γ_i are the direction cosines. In order to satisfy $p^\mu p_\mu=0$,

$$e^2=1-h_{ij}\gamma_i\gamma_j , \quad \text{(A3)}$$

to first order.

The equations of motion for the photons are [41]

$$\frac{dp_\alpha}{dt}=\frac{1}{2}\partial_\alpha g_{\mu\nu}\frac{p^\mu p^\nu}{p_0} . \quad \text{(A4)}$$

The general expression for the collisionless Boltzmann equation is

$$\frac{\partial f}{\partial t}+\frac{\partial f}{\partial x^i}\frac{dx^i}{dt}+\frac{\partial f}{\partial \gamma_i}\frac{d\gamma_i}{dt}+\frac{\partial f}{\partial p_0}\frac{dp_0}{dt}=0 . \quad \text{(A5)}$$

We integrate this equation over energy to obtain the equation for Δ, the brightness. Each term in the integral of (A5) is now discussed in turn.

1. Redshift term

The redshift term is

$$\frac{4\pi}{\mathcal{E}}\int p_0^3 dp_0 \frac{\partial f}{\partial p_0}\frac{dp_0}{dt}=4\frac{1}{a}\frac{da}{dt}(1+\Delta^{(1)}+\Delta^{(2)}) -2\gamma_i\gamma_j\frac{\partial h_{ij}}{\partial t}-2\gamma_i\gamma_j\frac{\partial h_{ij}^{(2)}}{\partial t} +\{-2\gamma_i\gamma_j\Delta^{(1)}-4h_{kj}\gamma_k\gamma_i +2h_{kl}\gamma_i\gamma_j\gamma_k\gamma_l\}\frac{\partial h_{ij}}{\partial t} , \quad \text{(A6)}$$

where $\mathcal{E}$ is the average energy density of the photons. The first term represents the universal redshift due to the expansion. Note that the brightness fluctuation is independent of the redshift factor since all photons redshift in the same manner. Thus, the term from the explicit time dependence of the spectrum will cancel the first term (see part 4). The other terms represent gravitational redshifts due to perturbations of the metric.

2. Anisotropy term

Anisotropy is generated as a first-order gravitational effect due to gravitational redshifts from overdense regions, i.e., the Sachs-Wolfe effect [42]. Therefore $\partial f/\partial\gamma_i$ has a contribution to first order in the metric perturbations. Gravitational lensing, $d\gamma_i/dt$, is also a first-order effect. Thus the whole term is second order:

$$\frac{4\pi}{\mathcal{E}}\int p_0^3 dp_0 \frac{\partial f}{\partial \gamma_i}\frac{d\gamma_i}{dt}=\frac{\partial\Delta^{(1)}}{\partial\gamma_i}\frac{1}{2}\left\{\frac{\partial h_{jk}}{\partial t}\gamma_i\gamma_j\gamma_k +\frac{1}{a}\partial_i h_{jk}\gamma_j\gamma_k\right\} . \quad \text{(A7)}$$

3. Inhomogeneity term

The inhomogeneity term is

$$\frac{4\pi}{\mathcal{E}}\int p_0^3 dp_0 \frac{\partial f}{\partial x^i}\frac{dx^i}{dt}=\frac{\gamma_i}{a}\left\{\frac{\partial\Delta^{(1)}}{\partial x^i}+\frac{\partial\Delta^{(2)}}{\partial x^i}\right\} +\frac{1}{a}\frac{\partial\Delta^{(1)}}{\partial x^i}\left[h_{ij}\gamma_j-\frac{1}{2}h_{jk}\gamma_j\gamma_k\gamma_i\right] . \quad \text{(A8)}$$

This term represents the effects of a spatially dependent perturbation in the photon energy density. The first term has no dependence on the metric fluctuations and is the flat space approximation used in Eq. (23). The second term represents corrections due to the mass shell constraint, Eqs. (A2) and (A3).

4. Explicit time dependence term

The explicit time dependence term is

$$\frac{4\pi}{\mathcal{E}}\int p_0^3 dp_0 \frac{\partial f}{\partial t}=-4\frac{1}{a}\frac{da}{dt}(1+\Delta^{(1)}+\Delta^{(2)}) +\frac{\partial\Delta^{(1)}}{\partial t}+\frac{\partial\Delta^{(2)}}{\partial t} . \quad \text{(A9)}$$

The first term represents the uniform redshift of the spectrum. It cancels with the energy redshift leaving no effect on temperature perturbations.

5. Complete first-order expression

Summing the above, we arrive at

$$\frac{\partial\Delta^{(1)}}{\partial t}+\frac{\gamma_i}{a}\frac{\partial\Delta^{(1)}}{\partial x^i}=2\gamma_i\gamma_j\frac{\partial h_{ij}}{\partial t} , \quad \text{(A10)}$$

to first order. This term represents the gravitational redshift of the photons due to the metric fluctuations and gives the conventional Sachs-Wolfe effect [43].

6. Complete second-order expression

In second order,

$$\frac{\partial\Delta^{(2)}}{\partial t}+\frac{\gamma_i}{a}\frac{\partial\Delta^{(2)}}{\partial x^i}=2\gamma_i\gamma_j\frac{\partial h_{ij}^{(2)}}{\partial t}+\{2\gamma_i\gamma_j\Delta^{(1)}+4h_{kj}\gamma_k\gamma_i-2h_{kl}\gamma_i\gamma_j\gamma_k\gamma_l\}\frac{\partial h_{ij}}{\partial t} -\frac{\partial\Delta^{(1)}}{\partial\gamma_i}\frac{1}{2}\left\{\frac{\partial h_{jk}}{\partial t}\gamma_i\gamma_j\gamma_k+\frac{1}{a}\partial_i h_{jk}\gamma_j\gamma_k\right\}-\frac{1}{a}\left\{\frac{\partial\Delta^{(1)}}{\partial x^i}\left[h_{ij}\gamma_j-\frac{1}{2}h_{jk}\gamma_j\gamma_k\gamma_i\right]\right\} . \quad \text{(A11)}$$

This expression gives the second-order Sachs-Wolfe effect and gravitational lensing effects.

APPENDIX B: COMPTON COLLISION TERM

Here we present the general expansion of Eq. (3) to second order, and give the explicit sources in the collision term of Eq. (6). First we must express the matrix element in the frame of the radiation background:

$$|M|^2=(4\pi)^2\alpha^2 2\left\{(1+\cos^2\beta)-2\cos\beta(1-\cos\beta)\left[\frac{\mathbf{q}\cdot\mathbf{p}}{mp}+\frac{\mathbf{q}\cdot\mathbf{p}'}{mp'}\right]+(1-\cos\beta)^2\frac{p^2}{m^2}+\frac{q^2}{m^2}\cos\beta(1-\cos\beta)\right.$$
$$\left.+(1-\cos\beta)(1-3\cos\beta)\left[\frac{\mathbf{q}\cdot\mathbf{p}}{mp}+\frac{\mathbf{q}\cdot\mathbf{p}'}{mp'}\right]^2+2\cos\beta(1-\cos\beta)\frac{(\mathbf{q}\cdot\mathbf{p})(\mathbf{q}\cdot\mathbf{p}')}{m^2pp'}\right\}+\text{h.o.}\ , \tag{B1}$$

where higher order (h.o.) represents third and higher order in v and p/m. The following identities are very useful for the calculation. Expansion to second order in energy transfer can be handled in a quite compact way by denoting it as an expansion in $\delta p=q-q'$ of the delta function for energy conservation:

$$\delta(p+q-p'-q')=\delta(p-p')+\frac{1}{2m}\{2(\mathbf{p}-\mathbf{p}')\cdot\mathbf{q}+(\mathbf{p}-\mathbf{p}')^2\}\left[\frac{\partial}{\partial p'}\delta(p-p')\right]$$
$$+\frac{1}{8m^2}\{2(\mathbf{p}-\mathbf{p}')\cdot\mathbf{q}+(\mathbf{p}-\mathbf{p}')^2\}^2\left[\frac{\partial^2}{\partial p'^2}\delta(p-p')\right]+\text{h.o.}\ , \tag{B2}$$

which is of course defined and justified by integration by parts. Integrals over the electron distribution function are trivial:

$$\int\frac{d^3\mathbf{q}}{(2\pi)^3}g(\mathbf{q})=n_e\ ,$$
$$\int\frac{d^3\mathbf{q}}{(2\pi)^3}q_ig(\mathbf{q})=mv_in_e\ , \tag{B3}$$
$$\int\frac{d^3\mathbf{q}}{(2\pi)^3}q_iq_jg(\mathbf{q})=m^2v_iv_jn_e+mT_e\delta_{ij}n_e\ .$$

Now we substitute all of this into the general collision equation (3) and obtain the explicit expressions for the terms of Eq. (6):

$$C_0=\delta(p-p')(1+\cos^2\beta)F_1(\mathbf{x},\mathbf{p},\mathbf{p}')\ ,$$
$$C_v=\left\{\left[\frac{\partial}{\partial p'}\delta(p-p')\right](1+\cos^2\beta)\mathbf{v}\cdot(\mathbf{p}-\mathbf{p}')-\delta(p-p')2\cos\beta(1-\cos\beta)\left[\frac{\mathbf{v}\cdot\mathbf{p}}{p}+\frac{\mathbf{v}\cdot\mathbf{p}'}{p'}\right]\right\}F_1(\mathbf{x},\mathbf{p},\mathbf{p}')\ ,$$
$$C_{vv}=\frac{1}{2}\left[\frac{\partial^2}{\partial p'^2}\delta(p-p')\right](1+\cos^2\beta)[\mathbf{v}\cdot(\mathbf{p}-\mathbf{p}')]^2F_1(\mathbf{x},\mathbf{p},\mathbf{p}')$$
$$-\left[\frac{\partial}{\partial p'}\delta(p-p')\right]2\cos\beta(1-\cos\beta)\left[\frac{\mathbf{v}\cdot\mathbf{p}}{p}+\frac{\mathbf{v}\cdot\mathbf{p}'}{p'}\right]\mathbf{v}\cdot(\mathbf{p}-\mathbf{p}')F_1(\mathbf{x},\mathbf{p},\mathbf{p}')$$
$$+\delta(p-p')\left\{-(1-2\cos\beta+3\cos^2\beta)v^2+2\cos\beta(1-\cos\beta)\frac{(\mathbf{v}\cdot\mathbf{p})(\mathbf{v}\cdot\mathbf{p}')}{pp'}\right.$$
$$\left.+(1-\cos\beta)(1-3\cos\beta)\left[\frac{\mathbf{v}\cdot\mathbf{p}}{p}+\frac{\mathbf{v}\cdot\mathbf{p}'}{p'}\right]^2\right\}F_1(\mathbf{x},\mathbf{p},\mathbf{p}')\ , \tag{B4}$$
$$C_{p/m}=-\left[\frac{\partial}{\partial p'}\delta(p-p')\right](1+\cos^2\beta)\frac{(\mathbf{p}-\mathbf{p}')^2}{2m}F_2(\mathbf{x},\mathbf{p},\mathbf{p}')\ ,$$
$$C_{T_e/m}=\left\{\left[\frac{\partial^2}{\partial p'^2}\delta(p-p')\right](1+\partial\cos^2\beta)\frac{(\mathbf{p}-\mathbf{p}')^2}{2}-\left[\frac{\partial}{\partial p'}\delta(p-p')\right]2\cos\beta(1-\cos^2\beta)(p-p')\right.$$
$$\left.+\delta(p-p')[4\cos^3\beta-9\cos^2\beta-1]\right\}\frac{T_e}{m}F_1(\mathbf{x},\mathbf{p},\mathbf{p}')\ ,$$

and the higher-order terms,

$$
\begin{aligned}
C_{vp/m} = &-\left[\frac{\partial^2}{\partial p'^2}\delta(p-p')\right](1+\cos^2\beta)(\mathbf{p}-\mathbf{p}')^2\frac{\mathbf{v}\cdot(\mathbf{p}-\mathbf{p}')}{2m}F_2(\mathbf{x},\mathbf{p},\mathbf{p}') \\
&+\left[\frac{\partial}{\partial p'}\delta(p-p')\right]\left\{2\cos\beta(1-\cos^2\beta)(p-p')\frac{\mathbf{v}\cdot(\mathbf{p}-\mathbf{p}')}{m}F_3(\mathbf{x},\mathbf{p},\mathbf{p}')\right. \\
&\qquad\left.+\cos\beta(1-\cos\beta)(\mathbf{p}-\mathbf{p}')^2\left[\frac{\mathbf{v}\cdot\mathbf{p}}{mp}+\frac{\mathbf{v}\cdot\mathbf{p}'}{mp'}\right]F_2(\mathbf{x},\mathbf{p},\mathbf{p}')\right\} \\
&+\delta(p-p')\left\{\frac{\mathbf{v}\cdot(\mathbf{p}-\mathbf{p}')}{m}[2(1-2\cos\beta+3\cos^2\beta)F_3(\mathbf{x},\mathbf{p},\mathbf{p}')-(1+\cos^2\beta)F_1(\mathbf{x},\mathbf{p},\mathbf{p}')]\right. \\
&\qquad\left.-2\cos\beta(1-\cos\beta)\left[\left[\frac{p}{p'}-\cos\beta\right]\frac{\mathbf{v}\cdot\mathbf{p}'}{m}-\left[\frac{p'}{p}-\cos\beta\right]\frac{\mathbf{v}\cdot\mathbf{p}}{m}\right]F_3(\mathbf{x},\mathbf{p},\mathbf{p}')\right\}, \\
C_{(p/m)^2} = &\left[\frac{\partial^2}{\partial p'^2}\delta(p-p')\right](1+\cos^2\beta)\frac{(\mathbf{p}-\mathbf{p}')^4}{2m^2}\left[\frac{1}{4}F_1(\mathbf{x},\mathbf{p},\mathbf{p}')+F_3(\mathbf{x},\mathbf{p},\mathbf{p}')\right] \\
&-\left[\frac{\partial}{\partial p'}\delta(p-p')\right]2\cos\beta(1-\cos^2\beta)(p-p')\frac{(\mathbf{p}-\mathbf{p}')^2}{2m^2}F_3(\mathbf{x},\mathbf{p},\mathbf{p}') \\
&+\delta(p-p')\left\{(1-\cos\beta)^2\left[\frac{p}{m}\right]^2F_1(\mathbf{x},\mathbf{p},\mathbf{p}')+(1+\cos^2\beta)\frac{(\mathbf{p}-\mathbf{p}')^2}{2m^2}F_2(\mathbf{x},\mathbf{p},\mathbf{p}')\right. \\
&\qquad-2\cos\beta(1-\cos\beta)\frac{(p-p'\cos\beta)(p'-p\cos\beta)}{m^2}F_3(\mathbf{x},\mathbf{p},\mathbf{p}') \\
&\qquad\left.-[1-2\cos\beta+3\cos^2\beta]\frac{(\mathbf{p}-\mathbf{p}')^2}{m^2}F_3(\mathbf{x},\mathbf{p},\mathbf{p}')\right\},
\end{aligned}
\tag{B5}
$$

where we have written

$$
\begin{aligned}
F_1(\mathbf{x},\mathbf{p},\mathbf{p}') &= f(\mathbf{x},\mathbf{p}')-f(\mathbf{x},\mathbf{p}), \\
F_2(\mathbf{x},\mathbf{p},\mathbf{p}') &= f(\mathbf{x},\mathbf{p})+2f(\mathbf{x},\mathbf{p})f(\mathbf{x},\mathbf{p}')+f(\mathbf{x},\mathbf{p}'), \\
F_3(\mathbf{x},\mathbf{p},\mathbf{p}') &= f(\mathbf{x},\mathbf{p}')[1+f(\mathbf{x},\mathbf{p})]
\end{aligned}
\tag{B6}
$$

for compactness.

[1] C. J. Hogan, N. Kaiser, and M. J. Rees, Philos. Trans. R. Soc. London **307**, 97 (1982).
[2] G. F. Smoot *et al.*, Astrophys. J. Lett. **396**, L1 (1992).
[3] T. Gaier *et al.*, Astrophys. J. Lett. **398**, L1 (1992).
[4] J. P. Ostriker and E. T. Vishniac, Astrophys. J. Lett. **306**, L51 (1986).
[5] E. T. Vishniac, Astrophys. J. **322**, 597 (1987).
[6] G. Efstathiou, in *Large Scale Motions in the Universe: A Vatican Study Week,* edited by V. C. Rubin and G. V. Coyne (Princeton University, Princeton, NJ, 1988), p. 299.
[7] R. Subrahmanyan *et al.*, Mon. Not. R. Astron. Soc. **263**, 416 (1993).
[8] J. R. Bond and G. Efstathiou, Mon. Not. R. Astron. Soc. **226**, 665 (1987).
[9] N. Kaiser, Mon. Not. R. Astron. Soc. **202**, 1169 (1983).
[10] J. Bernstein, *Relativistic Kinetic Theory* (Cambridge University Press, Cambridge, England, 1988). This approach was suggested to us by S. Dodelson. See also S. Dodelson and J. Jubas, Astrophys. J. (to be published).
[11] F. Mandl and G. Shaw, *Quantum Field Theory* (Wiley, New York, 1984), p. 157.
[12] Ya. B. Zel'dovich, A. F. Illarionov, and R. A. Sunyaev, Zh. Eksp. Teor. Fiz. **62**, 1217 (1972) [Sov. Phys. JETP **35**, 643 (1972)].
[13] N. Kaiser, Astrophys. J. **282**, 374 (1984).
[14] R. A. Sunyaev and Ya. B. Zel'dovich, Comments Astrophys. Space Phys. **4**, 79 (1972).
[15] A. S. Kompaneets, Zh. Eksp. Teor. Fiz. **31**, 876 (1957) [Sov. Phys. JETP **4**, 730 (1957)].
[16] Ya. B. Zel'dovich and R. A. Sunyaev, Astrophys. Space Sci. **4**, 301 (1969).
[17] J. Bartlett and A. Stebbins, Astrophys. J. **371**, 8 (1991).
[18] G. F. Smoot *et al.*, Astrophys. J. Lett. **371**, L1 (1991).
[19] J. C. Mather *et al.*, Astrophys. J. Lett. (to be published).
[20] S. Cole and N. Kaiser, Mon. Not. R. Astron. Soc. **233**, 637 (1988); J. Bartlett and J. Silk (unpublished).
[21] N. Y. Gnedin and J. P. Ostriker, Astrophys. J. **400**, 1 (1992).
[22] Note that our definition of Δ does not exactly conform with the standard convention [6], where $\Delta=\delta f(T/4)(\partial\bar{f}/\partial T)\simeq 4[T_{\rm eff}(p)-T]/T$, with $\bar{f}$ a Planck distribution at the average temperature T and $T_{\rm eff}(p)$ the

effective temperature of the spectrum as a function of frequency. Under this definition, Δ retains spectral information. We define Δ as the perturbation in the total energy density, which is explicitly independent of frequency. The two definitions coincide for a uniform shift in the temperature (e.g., the linear Doppler effect), which is the situation usually considered. Care should therefore be taken in associating our Δ with temperature distortions [cf. Eq. (12)].

[23] J. R. Bond, in *The Early Universe,* edited by W. G. Unruh and G. W. Semenoff (Reidel, Dordrecht, Boston, 1988), p. 283.

[24] Notice that the effect of scattering in an inhomogeneously ionized medium may be treated in the same manner as the Vishniac effect.

[25] A. G. Doroshkevich, Ya. B. Zel'dovich, and R. A. Sunyaev, Astron. Zh. **55**, 913 (1978) [Sov. Astron. **22**, 523 (1978)].

[26] S. Weinberg, *Gravitation and Cosmology* (Wiley, New York, 1972).

[27] K. M. Gorski, R. Stompor, and R. Juszkiewicz, Astrophys. J. **410**, L1 (1993).

[28] S. Dodelson and J. M. Jubas, Phys. Rev. Lett. **70**, 2224 (1993).

[29] G. Efstathiou, J. R. Bond, and S. D. M. White, Mon. Not. R. Astron. Soc. **258**, 1p (1992).

[30] J. Holtzman, Astrophys. J. Suppl. **71**, 1 (1989). We have normalized to COBE [2].

[31] M. L. Wilson and J. Silk, Astrophys. J. **243**, 14 (1981).

[32] M. Tegmark and J. Silk, Astrophys. J. (to be published).

[33] N. Sugiyama, J. Silk, and N. Vittorio, Astrophys. J. Lett. (to be published).

[34] P. J. E. Peebles, Nature (London) **327**, 210 (1987).

[35] R. Cen, J. Ostriker, and P. J. E. Peebles, Astrophys. J. **415**, 423 (1993).

[36] E. Fomalont *et al.*, Astrophys. J. **404**, 8 (1993).

[37] A. C. S. Readhead *et al.*, Astrophys. J. **384**, 396 (1989).

[38] Determined from R. Subrahmanyan (private communication). This normalization comes from the relation $W_{\rm ATCA}(q)=[F(q)/(2\pi\phi_b\theta_b)]^2$ with ϕ_b and θ_b as the Gaussian widths of the synthesized beam in radians. $F(q)$ corresponds to the filter function defined in their Eq. (8) [7]. Note also that the effective Gaussian beam width of $\sigma=(\phi_b\theta_b)^{1/2}=0.87'$ is on a scale larger than that of the peak sensitivity $l=4500$. This is indicative of the non-Gaussian nature of their beam and should be taken as a warning that their upper limit cannot be easily translated into a constraint on $C(0,0.87')$; the true window function must be employed to compare with a theory.

[39] E. Martinez-Gonzalez, J. L. Sanz, and J. Silk, Phys. Rev. D **46**, 4193 (1992).

[40] A. Jaffe, A. Stebbins, and J. A. Frieman, Astrophys. J. (to be published).

[41] P. J. E. Peebles and J. T. Yu, Astrophys. J. **162**, 815 (1970).

[42] R. K. Sachs and A. M. Wolfe, Astrophys. J. **147**, 73 (1967).

[43] P. J. E. Peebles, *Large Scale Structure of the Universe* (Princeton University, Princeton, NJ, 1980), pp. 365–372.